U.S. DEPARTMENT OF THE INTERIOR
U.S. GEOLOGICAL SURVEY

# Zeolites and selected other hydrothermal minerals in the Cascade Mountains of northern Oregon

by Keith E. Bargar and Robert L. Oscarson

Open-File Report 97-100

This report is preliminary and has not been reviewed for conformity with U.S. Geological Survey editorial standards or with the North American Stratigraphic Code. Any use of trade, product or firm names is for descriptive purposes only and does not imply endorsement by the U.S. Government.

U.S. Geological Survey, 345 Middlefield Road, Menlo Park, CA 94025

CONTENTS



FIGURES

TABLES

## ABSTRACT

Twenty-three zeolite minerals were identified during secondary mineralogy studies of late Tertiary to Quaternary geothermal drill hole specimens and late Tertiary volcanic rock outcrop samples in three areas of the Oregon Cascade Mountains (near Mount Hood, Breitenbush-Austin Hot Springs area, and Newberry Volcano). The Neogene to Holocene volcanic rocks contain euhedral to subhedral zeolite crystals in open spaces of fractures, vesicles, and between breccia fragments. The widespread occurrence of zeolite minerals indicates that a substantial portion of these volcanic rocks underwent low-temperature (<200°C), zeolite-facies, hydrothermal alteration at some time following their emplacement. A few of the zeolites (wairakite, faujasite, ferrierite, harmotome, and yugawaralite) encountered during these studies are not previously reported elsewhere in Oregon.

Some low-temperature zeolite minerals are superimposed upon higher-temperature (relict) alteration minerals; the higher-temperature minerals undoubtedly formed during late cooling of scattered, late Miocene volcanic deposits in the Western Cascade Mountains of northern Oregon. The higher-temperature relict minerals (quartz, epidote, garnet, actinolite, magnetite, talc, corderite, adularia(?), and hornblende), exposed in halos surrounding the eroded intrusive centers of these ancient volcanoes, formed at temperatures up to ~400°C and are indicative of greenschist- to subgreenschist-facies metamorphism. Several associated clays, carbonates, silicas, sulfides, sulfates, iron oxides, and other minerals undoubtedly were produced over the zeolite to greenschist temperature range (~30° to 400°C).

Homogenization temperatures of fluid inclusions in quartz, calcite, and anhydrite from rock outcrop and geothermal drill holes are consistent with this temperature range. Most heating/freezing analyses indicate that the mineral-precipitating fluids were low salinity, low-temperature thermal waters compatible with zeolite-facies metamorphism. Fluid inclusions with higher homogenization temperatures (>200°C) were only encountered in the active Newberry volcano geothermal system and in the vicinity of small, late Tertiary intrusives in the Western Cascade Range of northern Oregon.

The studied late Tertiary volcanic rocks from the Breitenbush-Austin Hot Springs area and near Mount Hood (exclusive of greenschist metamorphic halos surrounding small, scattered intrusions) have primarily been subjected to low-temperature metamorphism. The distribution of secondary minerals in these two areas appear to be consistent with localized high heat-flow conditions rather than widespread high heat-flow conditions.

## INTRODUCTION

Quaternary volcanic activity, several hot springs, and a few fumaroles present in the Cascade Range of northern Oregon suggested the possibility that exploitable geothermal energy sources might occur within these mountains. During the 1970's and 1980's, numerous test drill holes were completed in several areas of the Cascades to aid in the evaluation of some of the more favorable geothermal sites. Detailed studies of hydrothermal alteration mineralogy were made for core and cuttings from twenty-four of the drill holes at Newberry volcano (Keith and Bargar, 1988; Bargar and Keith, in preparation), the Mount Hood area (Bargar, Keith, and Beeson, 1993), and the Breitenbush-Austin Hot Springs area (Bargar, 1990, 1994; Keith, 1988) (Figure 1).

Figure 1 near here

During the investigations, twenty-three zeolite minerals were identified, along with many other alteration minerals, in drill hole specimens from these three areas or in nearby outcrops of late Tertiary volcanic rocks at Mount Hood and the Breitenbush-Austin Hot Springs area.

Zeolite minerals are a large group of hydrated aluminosilicates that contain one or more alkali or alkaline earth cations (Mumpton, 1977). Zeolites can function as catalysts to promote chemical reactions; they have the unique ability to gain or lose liquids (generally water) and gases (such as ammonia); and they can act as cation exchangers without significant alteration of their structures (Barrer, 1978). Consequently, there are numerous commercial uses for both natural and synthetic zeolites ranging from additives for various types of pollution abatement, agriculture and aquiculture, energy conservation, metallurgy, and even as a polishing agent in toothpaste (Mumpton, 1978). No ore-grade zeolite deposits occur in the Cascade Mountains. Mining claims have been filed in several areas of eastern Oregon, although little or no zeolite ore has been extracted from these prospects (Mumpton, 1983).

Zeolite minerals form in a variety of low-temperature (mostly <200°C), water-rich environments including alkaline lakes, deep-sea sediments, cooling lava flows, and hydrothermal systems (Tschernich, 1992). Drill-hole and rock-outcrop specimens of late Tertiary to Holocene volcanic rocks (intrusives, lava flows, pyroclastic flows, and volcaniclastic deposits) from the northern Oregon Cascade Mountains (including Newberry volcano) contain sparse to common, subhedral to euhedral, zeolite crystals in open spaces of vesicles, fractures, and between fragments of volcanic or tectonic breccias. Although zeolitization can occur with diagenetic or deuteric alteration, the large size of the numerous euhedral zeolite crystals is believed to be an indication that these minerals precipitated from circulating hydrothermal fluids (Gottardi, 1989). Chemical composition of the zeolite minerals is somewhat variable and reflects the elements contained in the mineralizing solutions which in turn are influenced by the rocks through which the waters flow (Barrer, 1982).

Because of their unique properties, the large number of identified minerals, and their wide-spread abundance in the altered late Tertiary volcanic rocks, these zeolites constitute a significant mineral group in Oregon's Cascade Mountains. Unfortunately, they have been largely ignored by previous workers. Some studies list identified zeolite minerals (Hammond, Anderson, and Manning 1980), but many investigators just report that 'zeolites' were present in their studies. In part, the subordination of zeolite minerals has resulted from the difficulty in identifying individual members of this large mineral group (40+ species). In this report, we present information on the occurrence, morphology, and chemistry of many of the zeolites and other minerals that were encountered in studies of low-temperature hydrothermally altered volcanic rocks from three geothermal areas in the Oregon Cascade Mountains. A few of the zeolites discussed in this report (wairakite, faujasite, ferrierite, harmotome, and yugawaralite) do not appear to previously have been reported elsewhere in Oregon.

## Analytical Methods

A few zeolite minerals have distinctive morphologies or optical properties, and individual mineral identifications can be made by routine binocular or petrographic microscope methods. Most zeolites, however, can best be identified by X-ray diffraction (XRD) (a Norelco X-ray unit and Cu-K$\alpha$ radiation was used in this study). Qualitative chemical analyses were obtained for several zeolites and other minerals during scanning electron microscope (SEM) studies, using a Cambridge Stereoscan 250 scanning electron microscope equipped with an energy dispersive spectrometer (EDS). The SEM studies also provided much information on the paragenesis and morphology of the secondary minerals. Quantitative chemical analyses for several zeolites and other minerals were obtained using either an ARL-SEMQ electron microprobe or JEOL JXA-8900L electron probe microanalyzer. The microprobe data for the Mount Hood area, Breitenbush-Austin Hot Springs area, and Newberry volcano are reported in Bargar, Keith and Beeson (1993), Oscarson and Bargar (1996), Bargar and Keith (in preparation), respectively. Both natural and synthetic mineral standards were used. Instrument conditions employed for the

carbon-coated, polished, thin-sections or mounts containing zeolite (and other) minerals were quite variable and include: a sample current of 7.5 or 15.0 nA, a beam diameter of 15 to 25 μm, count times of 10 or 20 seconds, and an accelerating voltage of 15 kV. Double- or single-polished thick sections and cleavage chips of hydrothermal quartz and calcite were utilized for fluid inclusion studies using a Linkam THM 600 heating/freezing stage and TMS 90 controller.

## Geothermal Areas

### Breitenbush-Austin Hot Springs area

In the Breitenbush-Austin Hot Springs area chemical geothermometers for three groups of hot springs, discharging dilute NaCl or Na-Ca-Cl (minor K and traces of Mg) water, indicate that reservoir temperatures may be as high as 186°C (Ingebritsen, Sherrod, and Mariner, 1989; Ingebritsen, Mariner, and Sherrod, 1994). These workers also indicate that high heat flow (>100 $mW/m^2$) throughout the area emanates from the Quaternary volcanic arc ~10-15 km to the east. Boden (1985) reported zeolites (epistilbite, stilbite, laumontite, mesolite, analcime, and mordenite), silica minerals (cristobalite, and quartz), clays (smectite, celadonite, chlorite, and illite), carbonates (calcite, dolomite, and siderite), iron oxides (hematite, and magnetite), pyrite, epidote, and antigorite alteration minerals from three shallow (150 m) drill holes (bottom temperatures 18°-55°C) in Miocene microdiorite and extrusive andesitic rocks near Austin Hot Springs. Two deep drill holes in the area, designated as CTGH-1 (1463 m) and SUNEDCO 58-28 (2457 m), encountered temperatures of only about 96°C and 141°C, respectively (Blackwell and Steele, 1987; A.F. Waibel, unpublished data, 1982). In drill hole CTGH-1, dominantly basaltic drill core samples yielded abundant heulandite, clinoptilolite, and mordenite below about 900 m depth; at depths of about 600 to 900 m, some chabazite, analcime, and thomsonite, and minor erionite, mesolite (misidentified as scolecite), phillipsite, and wellsite were recognized (Bargar, 1990). Other secondary minerals identified in this drill hole include iron oxide, smectite, celadonite, cristobalite, chalcedony, quartz, and traces of native copper, calcite, apatite(?) and adularia(?) (Bargar, 1990). Seven zeolites and numerous other secondary minerals were identified in late Tertiary, mostly basaltic to andesitic, lava flows and tuffaceous drill cuttings from drill hole SUNEDCO 58-28. Many drill-hole specimens contain laumontite and heulandite; a few specimens contain stilbite/stellerite, or analcime, and traces of mordenite, epistilbite, and scolecite (Bargar, 1994). Other secondary minerals from this drill hole include calcite, siderite, sepiolite(?), celadonite, smectite, mixed-layer chlorite-smectite, chlorite, corrensite(?), illite, cristobalite, chalcedony, quartz, chalcopyrite, pyrite, epidote, anhydrite, iron oxide, magnetite, and a serpentine-kaolinite mineral (Bargar, 1994). Several zeolites (analcime, chabazite, heulandite, epistilbite, gismondine, laumontite, levyne, mesolite, mordenite, phillipsite, scolecite, stilbite/stellerite, thomsonite, and yugawaralite) and other secondary clay (halloysite, kaolinite, smectite, illite, chlorite, mixed-layer chlorite-smectite, mixed-layer illite-smectite, celadonite, and vermiculite), silica (opal, cristobalite, quartz, and chalcedony), sulfide ( pyrite, cinnabar, chalcopyrite, sphalerite, galena, and polybasite) carbonate (calcite, dolomite, and siderite), iron oxide (magnetite, and hematite) garnet, adularia, epidote, apophyllite, gypsum, hornblende, actinolite, talc, cordierite, and chrysocolla mineral specimens were collected from scattered outcrops of late Tertiary volcanic rocks in the Breitenbush-Austin Hot Springs area.

### Mount Hood area

In the Mount Hood area, a few thermal springs occur near the southern base of the mountain. The dominant cation in the dilute, tepid Swim Warm Springs is Na although substantial Mg, Ca, and K are present in the samples (Mariner and others, 1980). Most of

the 30 geothermal test drill holes in the Mount Hood area encountered only low-temperature marginally thermal fluids (<23°C); however, in four of the drill holes, bottom temperatures were between 60° and 113°C. Present-day zeolite-facies metamorphism could occur at these temperatures. However, all of the zeolite minerals (wairakite, chabazite, ferrierite, heulandite, laumontite, mordenite, scolecite, stilbite/stellerite, and harmotome), and most of the ~43 silica, carbonate, clay, sulfate, sulfide, iron oxide, iron hydroxide and other secondary minerals identified in fractures, vugs, and between breccia fragments of late Tertiary basaltic to dacitic volcanic rocks and quartz diorite or quartz monzonite intrusives from outcrops and 13 geothermal drill holes, are believed to have formed during earlier periods of hydrothermal metamorphism (Bargar, Keith, and Beeson, 1993).

### Newberry volcano

At Newberry volcano, temperatures as high as 265°C were measured in one of two holes spudded in the Holocene caldera deposits. Temperatures as high as 170°C were recorded in drill holes on the western flank of the volcano (Arestad, Potter, and Stewart, 1988). Dilute hot springs within the caldera contain varying proportions of Na, Ca, Mg, and K (Mariner and others, 1980). Zeolite minerals (chabazite, dachiardite, heulandite, laumontite, mordenite, and phillipsite) are sparsely distributed in four of the seven flank drill holes studied (Bargar and Keith, in preparation). Within the caldera, analcime, chabazite, erionite, faujasite, clinoptilolite, dachiardite, and mordenite occur in fractures, vugs, and spaces between breccia fragments and as alteration products of glass in drill-hole specimens of rhyolitic tuffaceous rocks and basaltic sediments (Keith and Bargar, 1988). Thirty nine calcium silicate hydrate, carbonate, clay, silica, sulfide, sulfate, iron oxide, iron hydroxide, and other secondary minerals were also identified in these drill holes (Keith and Bargar, 1988; Bargar and Keith, in preparation). Present-day temperatures at which the Newberry volcano zeolites occur are about 30° to 160°C (Bargar and Keith, in preparation). The maximum temperature at which a few of the other secondary minerals were found was as high as 265°C.

## ZEOLITE MINERALS

Many of the zeolite minerals included in this study occur rarely and are not well known. Accordingly, chemical formulas from definitive zeolite references (Gottardi and Galli, 1985; Tschernich, 1992) are given for each of the zeolites identified in this investigation.

**Analcime $Na_{16}(Al_{16}Si_{32}O_{96})\cdot 16H_2O$ and Wairakite $Ca_8(Al_{16}Si_{32}O_{96})\cdot 16H_2O$.** Analcime and wairakite in the Oregon Cascade Mountains usually occur as colorless, subhedral to euhedral, trapezohedral crystals that formed in open spaces of fractures and vugs or between breccia fragments (Figure 2). Analcime appears to be more

Figure 2 near here

common than wairakite, but this study suggests that neither mineral is especially plentiful in the northern Oregon Cascades. A continuous solid-solution series exists between the analcime and wairakite end members (Gottardi and Galli, 1985). In this report, the nomenclature of Tschernich (1992), which defines analcime as containing more than 50 percent Na and wairakite as containing more than 50 percent Ca, is used to distinguish between the two minerals. Distinction between the two end-member minerals also has been reported by Coombs (1955) based on minor differences in their XRD patterns; however, Tschernich (1992) (for reasons not provided) indicates that analcime and wairakite cannot be distinguished by XRD. In this report, we utilized both methods to distinguish between the two minerals. Microprobe analyses of two Mount Hood wairakites (Bargar, Keith, and

Beeson, 1993) show that one specimen is very near the stoichiometric composition for the mineral (Figure 3A); whereas, a second specimen contains substantially more potassium

Figure 3 near here

than previously has been reported for wairakite (Gottardi and Galli, 1985; Tschernich, 1992).

XRD and semiquantitative SEM chemical data suggested that a "calcian" analcime mineral was present in the CTGH-1 drill hole near Breitenbush Hot Springs (Bargar, 1990). Subsequent electron microprobe analyses (Oscarson and Bargar, 1996), however, show that the mineral contains slightly more calcium than sodium (Figure 3A) and should more appropriately be classified as a "sodian" wairakite using nomenclature favored by Tschernich (1992). These microprobe analyses also show the presence of significant potassium (Figure 3A). Analcime specimens collected from the SUNEDCO 58-28 drill hole and outcrops near Breitenbush Hot Springs mostly are a nearly pure analcime end member (Bargar, 1994); one analysis shows the presence of a "calcian" analcime (Figure 3A).

The two intracaldera drill holes (USGS-N2 and RDO-1) at Newberry volcano both contain analcime (Keith and others, 1986; Keith and Bargar, 1988). Microprobe analyses for two specimens from depths of 314.6-315.1 m and 318.5 m in USGS-N2 show a pure end-member analcime and a "calcian" analcime containing significant potassium (Bargar and Keith, in preparation) (Figure 3A).

Analcime is a fairly common zeolite mineral that is found in many different environments including geothermal areas throughout the world where it formed at temperatures ranging from about 60° to 300°C (Kristmannsdóttir and Tómasson, 1978). Tschernich (1992) lists many localities in Oregon where analcime previously has been found. Wairakite also has been reported from geothermal areas in many parts of the world at about the same temperatures as analcime, but the mineral previously does not appear to have been located anywhere in Oregon (Tschernich, 1992).

**Chabazite $Ca_2(Al_4Si_8O_{24})\cdot 12H_2O$.** Colorless to white, euhedral, pseudocubic rhombohedral, chabazite crystals (Figure 4A) were identified in open-space

Figure 4 near here

deposits of specimens from several drill holes and outcrops at Mount Hood and the Breitenbush-Austin Hot Springs area; trace amounts of chabazite with the same morphology also coat fractures in core from one drill hole on the southern flank of Newberry volcano. The USGS-N2 drill hole, within the caldera of Newberry volcano, contains colorless, intergrown, twinned, hexagonal, lens-shaped, phacolitic, chabazite crystals between depths of 308.9 and 318.5 m. This phacolitic habit (Figure 4B) apparently is uncommon in the Cascade Mountains; leastwise it was not observed elsewhere during this study.

The composition of chabazite is characteristically quite variable (Gottardi and Galli, 1985). Semiquantitative EDS analysis of chabazite from the Newberry volcano USGS-N2 drill hole shows the presence of Ca, K, and Na (in order of abundance) in addition to Si and Al (Bargar and Keith, in preparation). Numerous microprobe analyses of chabazite from near Mount Hood and the Breitenbush-Austin hot-springs area (Figure 3B) show that calcium is the dominant cation in both areas; however, the Mount Hood chabazite contains substantial potassium (Bargar, Keith, and Beeson, 1993) while, in some chabazite from the Breitenbush-Austin area, sodium comprises as much as 50 percent of the exchangeable cations (Oscarson and Bargar, 1996).

Chabazite is a characteristic hydrothermal mineral in low-temperature (<75°C) alteration zones of Icelandic geothermal areas (Kristmannsdóttir and Tómasson, 1978).

Chabazite deposits in geothermal drill holes of the Cascade Mountains also occurs at similar low temperatures.

**Dachiardite** $(Na,K,Ca_{0.5})_4(Al_4Si_{20}O_{48})\cdot 18H_2O$. Dachiardite is a fairly rare zeolite mineral, but previously it has been identified from two locations in Oregon (Tschernich, 1992). At Newberry volcano, clusters of fibrous-, acicular-, or lath-shaped dachiardite crystals were found in a single specimen of rhyolitic tuff from 443.2-m depth (temperature ~98°C) in drill hole USGS-N2 where the mineral, along with smectite, formed by hydrothermal alteration of pumice fragments. A volcanic breccia specimen in drill hole GEO-N5 (southwest flank of Newberry volcano) contains tiny, colorless, dachiardite crystals along with mordenite and smectite in open spaces between breccia fragments at 886.7-m depth (temperature ~65°C).

Electron microprobe analyses of dachiardite from USGS-N2 (Bargar and Keith, in preparation) show that the mineral is rich in sodium (Figure 3C) and probably should be referred to as "sodium dachiardite" rather than just dachiardite as recommended by Bargar and others (1987). Bargar and others (1987) reported several optical, crystallographic, and chemical differences between dachiardite and sodium dachiardite.

**Epistilbite** $Ca_3(Al_6Si_{18}O_{48})\cdot 16H_2O$. Epistilbite was identified in four geothermal drill holes and one late Tertiary volcanic rock outcrop in the Mount Hood area (Bargar, Keith, and Beeson, 1993). Epistilbite occurs in drill cuttings of a basaltic intrusive specimen from 1,411-m depth in the SUNEDCO 58-28 hole (Bargar, 1994); this study also located minor epistilbite in seven outcrops of late Tertiary volcanic rocks in the Breitenbush-Austin Hot Springs area. Epistilbite has only been reported from two other areas in Oregon (Tschernich, 1992).

Electron microprobe analyses of the Mount Hood Ca-rich epistilbite indicate that it is lower in Si and higher in Al and Ca than the stoichiometric formula (Bargar, Keith, and Beeson, 1993). Analyzed specimens from the Breitenbush-Austin Hot Springs area plot into two groups with one group containing slightly more Na and a second group having substantially more K than the Mount Hood epistilbite (Oscarson and Bargar, 1996) (Figure 5A).

Figure 5 near here

**Erionite** $NaK_2MgCa_{1.5}(Al_8Si_{28}O_{72})\cdot 28H_2O$. Three specimens between 886 and 888 m depth in the CTGH-1 hole contain columnar bundles of acicular erionite crystals that formed later than smectite. SEM studies show that the erionite columns occasionally have hexagonal cross sections (Figure 6). Bundles of tiny prismatic erionite

Figure 6 near here

crystals occur in three basaltic sediment samples between depths of 315 and 318.5 m in the USGS-N2 hole. Temperatures at the depths where erionite occurs in the two geothermal holes were about 50°C. Electron microprobe analyses for erionite from the CTGH-1 hole show that the mineral contains nearly equal parts of Ca, Na, and K (Oscarson and Bargar, 1996) (Figure 5B).

**Faujasite** $Na_{20}Ca_{12}Mg_8(Al_{60}Si_{132}O_{384})\cdot 235H_2O$. Faujasite is a rare zeolite mineral that was identified in colorless to white vein fillings and intergranular open-space fillings of eleven porous basalt sediment specimens between 308.9 and 320 m depth in the USGS-N2 geothermal hole (temperature about 40° to 50°C) (Bargar and Keith, in preparation). SEM studies of the faujasite show extensive deterioration with cracking and flaking of the crystal surfaces (due to dehydration?) (Figure 7). Electron microprobe

Figure 7 near here

analyses of three faujasite crystals from 314.4 m depth show considerable variability in the Na and Ca contents (Figure 5C) (Bargar and Keith, in preparation) which is reported as typical for faujasite (Gottardi and Galli, 1985). To the best of our knowledge, this is the only faujasite ever reported from Oregon.

**Ferrierite $(Na,K)Mg_2Ca_{0.5}(Al_6Si_{30}O_{72})\cdot 20H_2O$.** Another rare zeolite mineral that previously has not been reported from Oregon is ferrierite. One fault gouge sample from a late Miocene andesite flow at the southern base of Mount Hood contained colorless, acicular to lamellar crystals of ferrierite in association with smectite (Figure 8)

Figure 8 near here

(Bargar, Keith, and Beeson, 1993). Electron microprobe analyses (Oscarson and Bargar, 1996) show the presence of significant Mg (Figure 5D) (Mg:Ca ranges from 3:1 to 6:1); ferrierite is one of the few zeolite minerals that may contain an appreciable amount of magnesium (about the same proportion as shown in the above formula) (Gottardi and Galli, 1985).

**Gismondine $Ca_4(Al_8Si_8O_{32})\cdot 16H_2O$.** Tschernich and Howard (1988) described gismondine filling vesicles, in association with chabazite, calcite, levyne, smectite, and thomsonite, in an outcrop of light colored volcanic rocks along the Oak Grove Fork of the Clackamas River in the Breitenbush-Austin Hot Springs area. A vesicular basaltic lava flow specimen was collected from the same general area for the present study. Vesicles in this specimen are filled by pseudotetragonal gismondine crystals and later chabazite (Figure 9). A scanning electron microscope EDS analysis of the

Figure 9 near here

gismondine shows only Ca, Al, and Si (Oscarson and Bargar, 1996). According to Tschernich (1992), the Oak Grove Fork area is the only location in the Pacific Northwest where gismondine has been found.

**Harmotome $Ba_2(Ca_{0.5},Na)(Al_5Si_{11}O_{32})\cdot 12H_2O$, Phillipsite $K_2(Ca_{0.5},Na)_4(Al_6Si_{10}O_{32})\cdot 12H_2O$, and Wellsite $(Ba,Ca,K_2)Al_2Si_6O_{16}\cdot 6H_2O$.** The three zeolite minerals, harmotome, phillipsite, and wellsite, are generally classified as belonging to the phillipsite-harmotome group of zeolite minerals (Gottardi and Galli, 1985). A single specimen of harmotome was collected from a tailings pile in an old mining area southwest of Mount Hood (Bargar, Keith, and Beeson, 1993); the colorless, blocky, hydrothermal, harmotome crystals (Figure 10A) formed in association with earlier

Figure 10 near here

stilbite/stellerite, (chlorite, pyrite, and calcite also are present) on a fracture surface of a late Tertiary andesite lava flow (Bargar, Keith, and Beeson, 1993). Electron microprobe analyses (Bargar, Keith, and Beeson, 1993) show that the euhedral, pseudo-orthorhombic, harmotome crystals have a very high Ba content (only minor Ca, Na, and K) (Figure 11A)

Figure 11 near here

which is characteristic of harmotome (Gottardi and Galli, 1985). Harmotome is an uncommon mineral and it does not appear to have been reported elsewhere in Oregon (Tschernich, 1992). Although harmotome has not been identified in modern geothermal areas, some harmotome is known to have a hydrothermal origin, (Tschernich, 1992).

Phillipsite occurs at several localities in Oregon (Tschernich, 1992). However, in the present study, phillipsite was identified only in two Breitenbush-Austin Hot Springs area outcrop samples and three core specimens from the CTGH-1 hole (Bargar, 1990). Phillipsite, an early-formed mineral in this drill core, occurs at depths of 811, 812, and 821 m (measured temperature ~40°C) as fillings in basalt vesicles or between fragments in volcanic breccia. Phillipsite from Icelandic geothermal areas occurs at temperatures between 60° and 85°C; Gottardi and Galli (1985), however, indicate that it can form at temperatures up to 200°C. The blocky to prismatic crystals occur in very closely spaced clusters (Figure 10B). At 812 m depth the phillipsite crystals have a skeletal appearance and are partly dissolved. The dominant cation in one CTGH-1 specimen is K (Figure 11A); Na and Ca (uncombined) are less abundant and Ba is absent.

Wellsite generally is defined as a barian phillipsite or as an intermediate member of the phillipsite-harmotome group. However, it is not clear if wellsite should be considered as a separate mineral. A thorough review of wellsite characteristics by Cerny, Rinaldi, and Surdam (1977) did not resolve the question. Tschernich (1992) recommends abandoning the term wellsite, and using phillipsite if the phillipsite-harmotome group mineral contains less than 50% Ba and harmotome if the mineral has more than 50% Ba. In this report, we retained the term wellsite because it is still recognized as a mineral name by the International Mineralogical Association (Tschernich, 1992).

Wellsite was identified only in vesicles of basaltic core from 564 m depth in the CTGH-1 hole (measured temperature is ~32°C). The mineral formed as randomly oriented, elongate, prismatic crystals (Figure 10C); clusters of radiating crystals; or closely spaced elongate crystals deposited as overlapping, radiating, hemispherical crystal clusters producing a botryoidal-appearing vesicle coating similar to phillipsite in Figure 10B. Electron microprobe analyses of the CTGH-1 wellsite (Oscarson and Bargar, 1996) shows that the mineral is composed of nearly equal amounts of Na and K+Ba, and contains relatively little Ca (Figure 11B). Tschernich (1992) indicates that "barian phillipsite (=wellsite)" occurs in at least two other locations in Oregon, both of which are only a few tens of kilometers from the CTGH-1 drill hole site.

**Heulandite $(Na,K)Ca_4(Al_9Si_{27}O_{72})\cdot 24H_2O$, and Clinoptilolite $(Na,K)_6(Al_6Si_{30}O_{72})\cdot 20H_2O$.** Heulandite group minerals—heulandite, clinoptilolite, and intermediate heulandite(?)—occur in drill holes and/or outcrops of all three areas studied. Researchers have distinguished between heulandite and clinoptilolite by either XRD (Mumpton, 1960) or chemical differences (Mason and Sand, 1960). Later studies (Alietti, 1972; Boles, 1972) even indicated the presence of a third or intermediate heulandite mineral phase. Reliance upon the definitions presented in the above references indicate that all three phases of the heulandite group of minerals are present in the Oregon Cascade Mountains. It should be noted, however, that recent texts on zeolite minerals indicate that there are uncertainties in the nomenclature of the mineral group (Gottardi and Galli, 1985) and it has been suggested that this group of minerals should be referred to simply as heulandite (Tschernich, 1992). In the present report, both heulandite and clinoptilolite (plus intermediate heulandite?) are used because there are definite differences in composition and(or) XRD characteristics of the minerals, and because, at the present time, the International Mineralogical Association recommends distinctions within the mineral group.

Heulandite was identified from fractures and open spaces between rock fragments in a few outcrops of late Tertiary volcanogenic deposits near Mount Hood; also, late Tertiary to Quaternary volcanic drill chips from five nearby geothermal holes contain tiny, colorless, tabular or blocky, heulandite crystals (Bargar, Keith, and Beeson, 1993).

Both heulandite and clinoptilolite are present in the lower part of the CTGH-1 drill hole near Breitenbush Hot Springs (Bargar, 1990). These heulandite group minerals were deposited in vesicles and fractures and between breccia fragments of late Tertiary andesitic

to basaltic lava flows, tuffs, and breccias. The tabular zeolite minerals formed later than hematite, most smectite, celadonite, and erionite but are earlier than cristobalite (Figure 12),

Figure 12 near here

mordenite, or minor late smectite.

Heulandite and intermediate heulandite(?) are fairly common minerals in open spaces of late Tertiary volcanic rocks throughout the Breitenbush-Austin Hot Springs area. Drill cutting specimens from several depths in the SUNEDCO 58-28 geothermal hole near Breitenbush Hot Springs also contain heulandite (Bargar, 1994).

Minor clinoptilolite occurs in rhyolitic tuff breccia core from near the middle of the USGS-N2 geothermal hole within the crater of Newberry volcano (Keith and Bargar, 1988). The only other heulandite group mineral identified from this volcano is a small amount of heulandite which occurs in fractures and vesicles of basaltic to andesitic drill core recovered from near the bottom of the western flank GEO-N5 hole (Bargar and Keith, in preparation).

Heulandite group minerals typically are found in modern geothermal areas at low to moderate temperatures. Measured temperatures at the depths where heulandite occurs in the SUNEDCO 58-28 drill hole range from about 80° to 130°C. These temperatures are within the apparent temperature limits (about 70° to 170°) for heulandite in Icelandic geothermal drill holes (Kristmansdóttir and Tómasson, 1978). However, some heulandite and clinoptilolite occur at temperatures as low as 30°C (range is about 30° to 96°C) in the CTGH-1 hole (Bargar, 1990). A bottom-hole temperature of about 60°C was measured for the only Mount Hood geothermal hole containing substantial heulandite (Bargar, Keith, and Beeson, 1993). At Newberry volcano, clinoptilolite was located in the USGS N2 drill hole at a depth where the measured temperature was about 99°C (Keith and Bargar, 1988); the present temperature at the core depth where heulandite was identified in the Newberry GEO-N5 hole is about 80°C (Bargar and Keith, in preparation).

Figure 13 shows a ternary diagram of the exchangeable cations commonly present

Figure 13 near here

in heulandite-group minerals of the northern Oregon Cascade Mountains. The Newberry and Breitenbush-Austin clinoptilolites are Na- or K-rich minerals that show no structural changes following heating at 450°C for 24 hours (Mumpton, 1960). One clinoptilolite specimen contains 8.34 wt. percent $K_2O$ (Bargar and Keith, in preparation). Clinoptilolites with such high $K_2O$ contents usually are produced by sedimentary (Stonecipher, 1978) or diagenetic (Ogihara and Iijima, 1990) processes rather than hydrothermal alteration. However, Keith, White, and Beeson (1978) and Bargar and Beeson (1985) reported $K_2O$ contents of 5.73 and 4.99 wt. percent, respectively for clinoptilolite in rhyolitic drill core specimens from thermal areas of Yellowstone National Park.

The remaining Breitenbush-Austin and Mount Hood heulandite group minerals show weak to substantial changes in intensity or spacing of XRD patterns following heating which correspond to results reported for heulandite or intermediate heulandite (Alietti, 1972; Boles, 1972). The microprobe analyses of these mineral specimens (Oscarson and Bargar, 1996) are all Ca-rich, but many of the analyses exhibit considerable scatter (Figure 13) owing to the presence of substantial Na or K.

**Laumontite $Ca_4(Al_8Si_{16}O_{48})\cdot 16H_2O$.** Laumontite is a common zeolite mineral in the Oregon Cascade Mountains. White, euhedral, prismatic, laumontite crystals, up to about 3 cm length, were found during this study filling open spaces between volcanic breccia fragments and lining vugs and fractures. Frequently, laumontite can be readily identified from its distinctive habit in which the terminal sloping {201} crystal face is prominent (Figure 14). Laumontite is readily dehydrated to form the mineral leonardite, a

Figure 14 near here

mineral name which Tschernich (1992) indicates should be discontinued and Gottardi and Galli (1985) view as only a variety of laumontite.

In the Mount Hood and the Breitenbush-Austin Hot Springs areas, laumontite occurs in several geothermal drill holes and numerous outcrops of late Tertiary volcanic rocks (Bargar, Keith, and Beeson, 1993; Bargar, 1994). The temperature range at which laumontite was identified in the SUNEDCO 58-28 hole is about 110° to 130°C. Conversely, at Newberry volcano, traces of laumontite were identified in only two drill holes (temperatures about 150° and 160°C) (Bargar and Keith, in preparation). These temperatures fall within the wide temperature range (43° to 230°C) at which laumontite previously has been reported (Kristmannsdóttir and Tómasson, 1978; McCulloh and others 1981).

Electron microprobe analyses of laumontite from both the Mount Hood and Breitenbush-Austin areas (Oscarson and Bargar, 1996) are Ca-rich with only minor amounts of other exchangeable cations (Figure 15A).

Figure 15 near here

**Levyne $NaCa_{2.5}(Al_6Si_{12}O_{36})\cdot 18H_2O$).** Levyne was found in association with smectite filling vesicles in a basalt outcrop located ~3-4 km southeast of Breitenbush Hot Springs. A fracture surface in the collected specimen was filled by thomsonite and chabazite. Levyne is not a rare mineral in Oregon, but it was not found elsewhere during the present study. In Iceland geothermal areas, levyne occurs at temperatures below 70°C (Kristmannsdóttir and Tómasson, 1978). In these Icelandic studies, chabazite forms over the same temperature range; however thomsonite occurs at temperatures as high as 110°C.

**Mesolite $Na_{16}Ca_{16}(Al_{48}Si_{72}O_{240})\cdot 64H_2O$ and Scolecite $Ca_8(Al_{16}Si_{24}O_{80})\cdot 24H_2O$.** Mesolite and scolecite are classified in the same group of fibrous zeolites (Figure 16) (Gottardi and Galli, 1985). Morphologically, the two minerals

Figure 16 near here

are indistinguishable; however, they can be differentiated by optical characteristics and they have different chemical compositions. Mesolite contains nearly equal proportions of Na and Ca, while Ca is the dominant cation in scolecite; other cations mostly are absent in both minerals (Figures 15B&C) (Tschernich, 1992). Analysis of trace elements for one scolecite specimen from the Mount Hood area shows the presence of minor Ba, Cu, Mn, Zn, and some Sr (Bargar, Keith, and Beeson, 1993).

Mesolite has been reported from several locations in Oregon including some areas within the Cascade Mountains; scolecite, on the other hand, has only been reported from three areas in Oregon (Tschernich, 1992). Mesolite and scolecite occur in only a few specimens collected for this study. Scolecite was reported from the CTGH-1 drill hole by Bargar (1990) based on EDS qualitative chemistry; however, subsequent electron microprobe analyses indicate that the mineral should have been identified as mesolite.

**Mordenite $Na_3KCa_2(Al_8Si_{40}O_{96})\cdot 28H_2O$).** Mordenite occurs in outcrop specimens and(or) drill hole samples in all three study areas, but it is not abundant in any of the areas (Keith and Bargar, 1988; Bargar, 1990; Bargar, Keith, and Beeson, 1993; Bargar, 1994). Individual white, fibrous to acicular, mordenite crystals or mattes of fibrous crystals (Figure 17) have a qualitative EDS chemistry consisting of Ca, Al, and Si,

Figure 17 near here

(Oscarson and Bargar, 1996) and, occasionally, trace amounts of Na or K. Mordenite usually formed later than associated hydrothermal minerals. Measured drill hole temperatures at depths in Cascade Range geothermal wells where mordenite was located range from abut 50° to more than 160°C; in Icelandic geothermal areas mordenite occurs over a somewhat wider temperature range (~75° to 230°C) (Kristmannsdóttir and Tómasson, 1978).

**Stilbite/Stellerite $NaCa_4(Al_9Si_{27}O_{72})\cdot 30H_2O$ / $Ca_4(Al_8Si_{28}O_{72})\cdot 28H_2O$.** Next to laumontite, white to colorless, tabular (Figures 18A&B) stilbite and stellerite are the

Figure 18 near here

most common zeolite minerals found in the Mount Hood and Breitenbush-Austin Hot Springs areas. These minerals were not identified in the Newberry volcano drill holes. The two solid-solution series minerals are combined here because they are distinguishable with confidence only by single-crystal XRD analysis (R.C. Erd, written communication, 1992) which was not attempted for this report. Electron microprobe analyses of stilbite/stellerite from the two study areas (Oscarson and Bargar, 1996) may show a separation of the two minerals (Figure 19A)

Figure 19 near here

with Na-rich analyses corresponding to stilbite; however, the possibility was not investigated for this report. Trace element analyses for two stilbite/stellerite specimens from the Mount Hood area show the presence of significant Pb (Bargar, Keith, and Beeson, 1993; Table 5). Drill-hole temperatures at depths where stilbite/stellerite was identified in SUNEDCO 58-28 were between 100° and 120°C (Bargar, 1994). Stilbite from Iceland geothermal drill holes occurs over a temperature range of 70° to about 170°C (Kristmannsdóttir and Tómasson, 1978). Tschernich (1992) lists several Oregon localities where stilbite previously has been reported. Tschernich regards stellerite as a variety of stilbite even though it is considered a separate mineral by the International Mineralogical Association.

**Thomsonite $Na_4Ca_8(Al_{20}Si_{20}O_{80})\cdot 24H_2O$.** Thomsonite was located in fracture and vesicle fillings between about 648 and 866 m depth in the CTGH-1 drill hole (temperatures between 30° and 50°C) (Bargar, 1990); bladed thomsonite (Figure 20) also fills vesicles and

Figure 20 near here

fractures of three outcrops in the Breitenbush-Austin Hot Springs area. While thomsonite is fairly rare in the three study areas of this report, it is not uncommon elsewhere in Oregon (Tschernich, 1992). Electron microprobe analyses (Oscarson and Bargar, 1996) for three thomsonite specimens appear to be fairly typical for thomsonite (Gottardi and Galli, 1985) (Figure 19B).

**Yugawaralite $Ca_2Al_4Si_{12}O_{32}\cdot 8H_2O$.** Rare specimens of yugawaralite are reported from a few geothermal areas where the temperatures range between 110° and 200°C (Gottardi and Galli, 1985; Tschernich, 1992). One sample, collected on the north shore of Detroit Reservoir, contains stacked, colorless, tabular, yugawaralite crystals, along with laumontite, stilbite/stellerite, scolecite, and mixed-layer chlorite-smectite in a very altered outcrop of very early Neogene (Hammond, Geyer, and Anderson, 1982) volcanic rocks. This occurrence appears to be the only specimen of yugawaralite that has ever been found in Oregon (Tschernich, 1992). Electron microprobe analyses of the mineral are given in Oscarson and Bargar (1996); calcium is the dominant cation (only minor sodium and potassium was detected) in these analyses (Figure 19C).

## OTHER MINERALS

Several hydrothermal alteration minerals, other than zeolites, were identified in the three study areas. Those from the Mt. Hood area and Newberry volcano drill holes have been discussed elsewhere (Bargar, Keith and Beeson, 1993; Bargar and Keith, 1984; Keith and Bargar, 1988; Bargar and Keith, in preparation). In the Breitenbush-Austin Hot Springs area several clay (smectite, chlorite, mixed-layer chlorite-smectite, kaolinite/serpentine, illite, mixed-layer illite-smectite, celadonite, vermiculite, and halloysite), carbonate (calcite, dolomite), silica (opal, cristobalite, chalcedony, and quartz), sulfide (pyrite, sphalerite, cinnabar, chalcopyrite, galena, and polybasite), sulfate (gypsum), iron oxide (amorphous, hematite, and magnetite), and other minerals (apophyllite, garnet, epidote, hornblende, chrysocolla, corderite, actinolite/tremolite, talc, copper, and adularia are found, sometimes in association with the zeolite minerals. Information on several of these minerals from the CTGH-1 and SUNEDCO 58-28 drill holes previously have been presented (Bargar, 1990; 1994). Detailed discussion of these minerals is not presented in this report; however, electron microprobe analyses and scanning electron microscope studies of a few selected minerals are briefly discussed.

**Actinolite/tremolite.** A fibrous, green amphibole collected from the Detroit Lake intrusive (Table 1 sample number 81 DL-2083B) is low in Fe and high in Mg and is probably

Table 1 near here

tremolite (optical characteristics were not checked). The other three analyzed samples given in Table 1 have quite variable compositions, but are consistent with actinolite (also the refractive index is >1.63).

**Adularia.** Only a single specimen containing adularia from the Breitenbush-Austin Hot Springs area was discovered during this investigation. Electron microprobe analyses of adularia crystals from a vein filling in a small intrusive ~7 kilometers northwest of Austin Hot Springs have fairly uniform compositions (Table 2). The adularia crystals were deposited later

Table 2 near here

than associated quartz (Figure 21). The SEM micrographs suggest that traces of a clay mineral

Figure 21 near here

may have formed later than the adularia, but no clay was identified by XRD.

**Apophyllite.** Euhedral apophyllite crystals (Figure 22) fill vesicles along with green

Figure 22 near here

smectite, analcime, chabazite, scolecite/mesolite, and stilbite/stellerite in one outcrop of late Tertiary volcanic rocks located ~7-8 kilometers south southeast of Mt. Jefferson. The only other apophyllite specimen located during these studies was in the USGS N2 drill hole (Keith and Bargar, 1988; Bargar and Keith, in preparation).

**Chlorite.** Figure 23 shows a rosette of sheet-like chlorite crystals. Chlorite group

Figure 23 near here

minerals are occasional hydrothermal alteration products in this study area; they occur in association with several other hydrothermal minerals, but generally do not appear to be associated with zeolite minerals. Microprobe analyses of chlorite from five samples collected in the Breitenbush-Austin Hot Springs area (Table 3) show significant variations in all of the

Table 3 near here

major elements (Si, Al, Fe, and Mg). Judging from the compositional differences shown in Table 3, it appears that two or more members of the chlorite group of minerals are present in this study area.

**Cinnabar.** A few abandoned cinnabar mines are located along the Oak Grove Fork of the Clackamas River about 4 kilometers north northwest of Austin Hot Springs. The deposits occur as fracture fillings in Miocene Columbia River Basalt (Brooks, 1963); the fractures (up to ~1.8 meters in width) (Brooks, 1963) mainly contain banded white-brown-black calcite with thin stringers of cinnabar (in one specimen collected for this study). According to Brooks (1963), the most productive cinnabar vein at one of the mines consists principally of stilbite and was called the "zeolite vein". The stilbite (or stellerite?) and associated cinnabar undoubtedly formed at temperatures less than ~200°C (Kristmannsdóttir and Tómasson, 1978). Euhedral to subhedral cinnabar crystals also were found in open space deposits with earlier-formed quartz (figure 24).

Figure 24 near here

**Dolomite.** Only a single dolomite specimen was collected from the Breitenbush-Austin Hot Springs area. The specimen containing wedge-shaped clusters of rhombic dolomite crystals (Figure 25) was found in the same locality as the above described cinnabar.

Figure 25 near here

**Epidote.** In the Breitenbush-Austin Hot Springs area, epidote occurs in association with a few small intrusives. Temperatures of epidote formation are reported to range between 200° and 250°C (Bird and others, 1984). Electron microprobe analyses of the subhedral to euhedral crystals (Figure 26) show differences in the iron and aluminum contents suggesting

Figure 26 near here

significant Fe-Al substitution (Table 4).

Table 4 near here

**Garnet.** Andradite garnet was collected from a few outcrops of Tertiary intrusives in the Breitenbush-Austin Hot Springs area. The dark brown, euhedral to subhedral, garnet crystals (Figure 27) probably formed at temperatures above 300°C (Bird and others, 1984),

Figure 27 near here

and were deposited in open spaces later than magnetite but earlier than epidote, quartz, scolecite, calcite, and chabazite in one specimen. Electron microprobe analyses of one dark brown garnet sample shows very high iron and extremely low aluminum contents (Table 5).

Table 5 near here

**Smectite.** Platy, green, clay minerals (smectite—Figure 28, chlorite, and mixed-layer

Figure 28 near here

chlorite-smectite), along with zeolites, are the most abundant hydrothermal alteration minerals in the three areas comprising this study. In the USGS Newberry 2 drill hole, smectite occurs at temperatures up to about 200°C; chlorite and mixed-layer chlorite-smectite are dominant at

higher temperatures (Keith and Bargar, 1988; Bargar and Keith, in preparation). Smectite in two rock outcrop samples contains much less magnesium than iron (Table 6). One specimen

Table 6 near here

of smectite from the CTGH-1 drill hole contains nearly equal proportions of iron and magnesium; however, a somewhat deeper smectite specimen has significantly greater magnesium content. Probably the smectite minerals analyzed ranged from nontronite to saponite.

## FLUID INCLUSIONS

Fluid inclusion data for the Mt. Hood drill hole and outcrop specimens and Newberry volcano drill hole samples are discussed elsewhere (Bargar, Keith and Beeson, 1993; Keith and Bargar, 1988; Bargar and Keith, in preparation). At Mt. Hood, the only drill hole or outcrop specimens suitable for fluid inclusion analysis were collected near late Tertiary intrusions. Homogenization temperatures for these fluid-inclusions averaged between 229° and 273°C and the inclusions must have formed during cooling of the nearby intrusions (Bargar, Keith and Beeson, 1993). High fluid-inclusion homogenization temperatures (exceeding the present-day reference surface boiling-point curve) for drill hole specimens from within the caldera of Newberry volcano drill holes are explained as resulting from pressures that were higher than at present because of an overlying deep lake at the time the fluid inclusions formed (Bargar and Keith, in preparation).

Fluid inclusion data (Table 7 and Figures 29 and 30A) for a few liquid-rich, mostly

Table 7 near here

Figures 29 and 30 near here

secondary, fluid inclusions in hydrothermal calcite, anhydrite, and primary quartz crystals (hydrothermal quartz in Figure 29 is not believed to be authigenic) from the SUNEDCO 58-28 drill hole in the Breitenbush-Austin Hot Springs area also have been presented (Bargar, 1993; 1994). These reports concluded that the minimum fluid-inclusion homogenization-temperature values at the sampled depths are consistent with the present-day measured temperatures within the drill hole, and that past temperatures in the rocks penetrated by the drill hole have been as much as ~75°C higher than the SUNEDCO 58-28 bottom-hole temperature measurements.

Table 7 also shows fluid inclusion data for several rock outcrop hydrothermal quartz and calcite specimens collected from the vicinity of Breitenbush Hot Springs (Figure 31).

Figure 31 near here

Homogenization-temperature values for hydrothermal quartz and calcite specimens from a region about 6-8 km northeast of the Detroit pluton are nearly all <200°C (Figure 30B) indicating that secondary mineralization of the late Tertiary volcanic rocks was produced by zeolite-facies alteration temperatures. Hydrothermal quartz specimen 81-82 was collected at the Detroit pluton where epidote, magnetite, actinolite, garnet, and chalcopyrite alteration minerals also occur. Homogenization-temperature values (181°-358°C) for this quartz specimen (Table 7, Figure 30C) are consistent with greenschist-facies temperatures produced during cooling of the intrusion. Secondary minerals characteristic of greater than zeolite-facies temperature metamorphism were not located in rock outcrop specimens (exclusive of dikes) collected between 1 and 6 kilometers northeast of the Detroit pluton. Late deposits of zeolites and other low-temperature hydrothermal alteration minerals are superimposed upon earlier higher-temperature hydrothermal minerals in exposures of the Detroit pluton and associated dikes.

## FINAL REMARKS

Twenty-three zeolite minerals were identified from rock outcrop and geothermal drill hole specimens obtained from the three study areas (near Mt. Hood, Newberry volcano, and the Breitenbush-Austin Hot Springs area). Of these zeolites, five (wairakite, faujasite, ferrierite, harmotome, and yugawaralite) have not been found elsewhere in Oregon. The widespread occurrence of zeolite minerals throughout the Western Cascade Mountains of northern Oregon (especially in the Breitenbush-Austin Hot Springs area) attests to the significance of zeolite metamorphism in altering the late Tertiary volcanic rocks.

The most intense (greenschist facies) hydrothermal alteration of volcanic rocks in the Mt. Hood and Breitenbush-Austin hot springs areas was observed in surface-exposed or drill-hole-penetrated, late Tertiary intrusions. A few kilometers away from these intrusions, zeolites and other low-temperature minerals are the dominant hydrothermal alteration products. The low-temperature minerals frequently are superimposed upon the higher-temperature minerals formed during late stages of hydrothermal alteration. Fluid inclusion data obtained for the two areas supports and serves to quantify these conclusions.

Within the caldera of the geothermally active Newberry volcano, fluid inclusion and hydrothermal mineralogy studies of the Quaternary volcanic drill hole specimens indicate that the rocks similarly have been altered by thermal fluids compatible with zeolite (at shallower levels) to greenschist (at depth) metamorphism. Drill holes located a few kilometers outside the caldera on the north, east, and south flanks of the volcano only contain evidence of very low temperature alteration. On the west flank of Newberry, the available measured temperature and fluid-inclusion homogenization temperature data suggest that the fluids become hotter nearer the rim of the caldera.

Preliminary hydrothermal alteration and fluid inclusion studies of geothermal drill holes at Medicine Lake volcano in northern California (Bargar, 1992; Bargar and Keith, 1993) also indicate that temperatures capable of producing greenschist-facies minerals appear to be confined to the area within the caldera. Like Newberry volcano, current available data for drill holes outside the caldera do not show evidence for high temperature alteration.

Two very different models have been proposed to explain the high heat flow observed throughout much of the Oregon Cascade Mountains. One model indicates that the source of the heat is widespread and that the geothermal energy potential of the area is very significant (Blackwell and others, 1990). The second model suggests that the heat source is more localized and the heat is spread by fluid movement resulting in a substantially smaller geothermal potential (Ingebritsen, Mariner, and Sherrod, 1994). The hydrothermal alteration studies conducted for this report appear to support the second model inasmuch as hydrothermal mineralogical evidence of past or present high temperatures in the Cascade Mountains of northern Oregon (and northern California) was found only in close proximity to small late Tertiary intrusions or within or very near the calderas of active volcanoes.

## ACKNOWLEDGMENTS

We thank the Oregon Department of Geology and Mineral Industries and A.F. Waibel for making drill hole samples available for this study. Reviews by M.A. Clynne and R.H. Mariner improved the manuscript and are gratefully acknowledged.

## REFERENCES

Alietti, Andrea, 1972, Polymorphism and crystal-chemistry of heulandites and clinoptilolites: American Mineralogist, v. 57, p. 1448-1462.

Arestad, J.F., Potter, R.W., II, and Stewart, G.E., 1988, Stratigraphic test drilling in the Newberry crater KGRA, Oregon: Geothermal Resources Council Bulletin, v. 17, no. 10, p. 3-8.

Bargar, K.E., 1990, Hydrothermal alteration in geothermal drill hole CTGH-1, High Cascade Range, Oregon: Oregon Geology, v. 52, no. 4, p. 75-81.
Bargar, K.E., 1992, Video-tape of bacteria-like moving particles in fluid inclusions from Medicine Lake Volcano, northern California (abs.): EOS, Transactions, American Geophysical Union, v. 73, no. 43, p. 640.
Bargar, K.E., 1993, Fluid-inclusion evidence for previous higher temperatures in the SUNEDCO 58-28 drill hole near Breitenbush Hot Springs, Oregon: Transactions, Geothermal Resources Council, v. 17, p. 83-89.
Bargar, 1994, Hydrothermal alteration in the SUNEDCO 58-28 geothermal drill hole near Breitenbush Hot Springs, Oregon: Oregon Geology, v. 56, no. 4, p. 75-87.
Bargar, K.E., and Beeson, M.H., 1985, Hydrothermal alteration in research drill hole Y-3, Lower Geyser Basin, Yellowstone National Park, Wyoming: U.S. Geological Survey Professional Paper 1054-C, 23 p.
Bargar, K.E., and Keith, T.E.C., 1984, Hydrothermal alteration mineralogy in Newberry 2 drill core, Newberry Volcano, Oregon: U.S. Geological Survey Open-File Report 84-92, 66 p.
Bargar, K.E., and Keith, T.E.C., 1993, Hydrothermal alteration in cores from geothermal drill holes at Medicine Lake Volcano, northeastern California (abs.): EOS, Transactions, American Geophysical Union, v. 74, no. 43, p. 688.
Bargar, K.E., and Keith, T.E.C., in prep., Hydrothermal mineralogy of core from geothermal drill holes at Newberry Volcano, Oregon: U.S. Geological Survey Bulletin, 290 p.
Bargar, K.E., Erd, R.C., Keith, T.E.C., and Beeson, M.H., 1987, Dachiardite from Yellowstone National Park, Wyoming: Canadian Mineralogist, v. 25, p. 475-483.
Bargar, K.E., Keith, T.E.C., and Beeson, M.H., 1993, Hydrothermal alteration in the Mount Hood area, Oregon: U.S. Geological Survey Bulletin 2054, 70 p.
Barrer, R.M., 1978, Zeolites and clay minerals as sorbents and molecular sieves: London, Academic Press, 497 p.
Barrer, R.M., 1982, Hydrothermal chemistry of zeolites: London, Academic Press, 360 p.
Bird, D.K., Schiffman, P., Elders, W.A., Williams, A.E., and McDowell, S.D., 1984, Calc-silicate mineralization in active geothermal systems: Economic Geology, v. 79, p. 671-695.
Blackwell, D.D., Black, G.L., and Priest, G.R., 1986, Geothermal-gradient data for Oregon (1982-1984): Oregon Department of Geology and Mineral Industries Open-File Report O-86-2, 107 p.
Blackwell, D.D., and Steele, J.L., 1987, Geothermal data from deep holes in the Oregon Cascade Range: Geothermal Resources Council Transactions, v. 11, p. 317-322.
Blackwell, D.D., Steele, J.L., Frohme, M.K., Murphy, C.F., Priest, G.R., and Black, G.L., 1990, Heat flow in the Oregon Cascade Range and its correlation with regional gravity, Curie point depths, and geology: Journal of Geophysical Research, v. 95, p. 19,495-19,516.
Boden, J.R., 1985, Lithology, hydrothermal petrology, and stable isotope geochemistry of three geothermal exploration drill holes, upper Clackamas River area, Cascade Range, Oregon: Riverside, University of California, unpub. MS thesis, 137 p.
Bodnar, R.J., and Sterner, S.M., 1984, Synthetic fluid inclusions in natural quartz I; compositional types synthesized and applications to experimental geochemistry: Geochimica et Cosmochimica Acta, v. 48, p. 2659-2668.
Boles, J.R., 1972, Composition, optical properties, cell dimensions, and thermal stability of some heulandite group zeolites: American Mineralogist, v. 57, p. 1463-1493.
Brooks, H.C., 1963, Quicksilver in Oregon: Oregon Department of Geology and Mineral Industries Bulletin 55, p. 105-111.
Cerny; P., Rinaldi, R., and Surdam, R.C., 1977, Wellsite and its status in the phillipsite-harmotome group: Neues Jahrbuch für Mineralogie Abhandlungen, v. 128, p. 312-330.

Coombs, D.S., 1955, X-ray observations on wairakite and non-cubic analcime: Mineralogical Magazine, v. 30, no. 230, p. 699-708.
Cummings, M.L., Pollock, J.M., Thompson, G.D., and Bull, M.K., 1990, Stratigraphic development and hydrothermal activity in the central Western Cascade Range, Oregon: Journal of Geophysical Research, v. 95, no. B12, p. 19,601-19,610.
Gottardi, Glauco, 1989, The genesis of zeolites: European Journal of Mineralogy, v. 1, p. 479-487.
Gottardi, Glauco and Galli, Ermanno, 1985, Natural Zeolites: Berlin, Springer-Verlag, 409 p.
Hammond, P.E., Anderson, J.L., and Manning, K.J., 1980, Guide to the geology of the Upper Clackamas and North Santiam Rivers area, northern Oregon Cascade Range, *in* Oles, K.F., Johnson, J.G., Niem, A.R., and Niem, W.A., eds., Geologic field trips in western Oregon and southwestern Washington: Oregon Department of Geology and Mineral Industries Bulletin 101, p. 133-167.
Hammond, P.E., Geyer, K.M., and Anderson, J.L., 1982, Preliminary geologic map and cross-sections of the upper Clackamas and North Santiam Rivers area, northern Oregon Cascade Range: Portland, Oregon, Portland State University Department of Earth Sciences, scale 1:62,500.
Ingebritsen, S.E., Mariner, R.H., and Sherrod, D.R., 1994, Hydrothermal systems of the Cascade Range, North-Central Oregon: U.S. Geological Survey Professional Paper 1044-L, 86 p.
Ingebritsen, S.E., Sherrod, D.R., and Mariner, R.H., 1989, Heat flow and hydrothermal circulation in the Cascade Range, north-central Oregon: Science, v. 243, p. 1458-1462.
Keith, T.E.C., 1988, Regional patterns of hydrothermal alteration, Breitenbush-Austin Hot Springs area, Cascade Range, Oregon, *in* Sherrod, D.R., ed., Geology and geothermal resources of the Breitenbush-Austin Hot Springs area, Clackamas and Marion Counties, Oregon: Oregon Department of Geology and Mineral Industries Open-File Report O-88-5, p. 31-37.
Keith, T.E.C., and Bargar, K.E., 1988, Petrology and hydrothermal mineralogy of U.S. Geological Survey Newberry 2 drill core from Newberry caldera, Oregon: Journal of Geophysical Research, v. 93, no. B9, p. 10,174-10,190.
Keith, T.E.C., White, D.E., and Beeson, M.H., 1978, Hydrothermal alteration and self-sealing in Y-7 and Y-8 drill holes in northern part of Upper Geyser Basin, Yellowstone National Park, Wyoming: U.S. Geological Survey Professional Paper 1054-A, p. A1-A26.
Keith, T.E.C., Gannett, M.W., Eichelberger, J.C., and Waibel, A.F., 1986, Lithology and hydrothermal alteration of drill hole RDO-1, Newberry caldera, Oregon: Oregon Geology, v. 48, no. 9, p. 103-107, 110.
Kristmannsdóttir, Hrefna, and Tómasson, Jens, 1978, Zeolite zones in geothermal areas in Iceland, *in* Sand, L.B., and Mumpton, F.A., eds., Natural Zeolites: Occurrence, Properties, Use: Oxford, Pergamon Press, p. 277-284.
Mariner, R.H., Swanson, J.R., Orris, G.J., Presser, T.S., and Evans, W.C., 1980, Chemical and isotopic data for water from thermal springs and wells of Oregon: U.S. Geological Survey Open-File Report 80-737, 50 p.
Mason, Brian, and Sand, L.B., 1960, Clinoptilolite from Patagonia. The relationship between clinoptilolite and heulandite: American Mineralogist, v. 45, p. 341-350.
McCulloh, T.H., Frizzell, V.A., Jr., Stewart, R.J., and Barnes, Ivan, 1981, Precipitation of laumontite with quartz, thenardite, and gypsum at Sespe Hot Springs, Western Transverse Ranges, California: Clays and Clay Minerals, v. 29, no. 5, p. 353-364.
Mumpton, F.A., 1960, Clinoptilolite redefined: American Mineralogist, v. 45, p. 351-369.
Mumpton, F.A., 1977, Natural zeolites, in Mumpton, F.A., ed., Mineralogy and geology of natural zeolites: Mineralogical Society of America Reviews in Mineralogy, v. 4, chapter 1, p. 1-17.

Mumpton, F.A., 1978, Natural zeolites: a new industrial mineral commodity, *in* Sand, L.B., and Mumpton, F.A., eds., Natural Zeolites: Occurrence, Properties, Use: Oxford, Pergamon Press, p. 3-27.

Mumpton, F.A., 1983, Discovery and commercial interest in zeolite deposits examined during Zeo-Trip '83, *in* Mumpton, F.A., ed., Zeo-Trip '83: An excursion to selected zeolite deposits in eastern Oregon, southwestern Idaho, and northwestern Nevada, and to the Tahoe-Truckee water reclamation plant, Truckee, California: International Committee on Natural Zeolites, July 7-10, 1983, Brockport, New York, p. 66-72.

Oscarson, R.L., and Bargar, K.E., 1996, Electron microprobe analyses of zeolite minerals from Neogene volcanic rocks in the Breitenbush-Austin Hot Springs area, Oregon: U.S. Geological Survey Open-File Report 96-41, 61 p.

Ogihara, Shigenori, and Iijima, Azuma, 1990, Exceptionally K-rich clinoptilolite—heulandite group zeolites from three offshore boreholes off northern Japan: European Journal of Mineralogy, v. 2, p. 819-826.

Pollock, J.M., and Cummings, M.L., 1985, North Santiam mining area, Western Cascades — relations between alteration and volcanic stratigraphy: Discussion and field trip guide: Oregon Geology, v. 47, no. 12, p. 139-145.

Roedder, Edwin, 1984, Fluid inclusions, *in* Ribbe, P.H., ed., Reviews in Mineralogy, v. 12: Washington, D.C., Mineralogical Society of America, 644 p.

Stonecipher, S.A., 1978, Chemistry of deep-sea phillipsite, clinoptilolite, and host sediments, in Sand, L.B., and Mumpton, F.A., eds., *in* Natural Zeolites: Occurrence, Properties, Use: Oxford, Pergamon Press, p. 221-234.

Tschernich, R.W., 1992, Zeolites of the World, Phoenix, Geoscience Press, Inc. 563 p.

Tschernich, R. W., and Howard, Donald, 1988, Gismondine from the Oak Grove Fork of the Clackamas River, Clackamas County, Oregon: Micro Probe, v. 6, no. 6, p. 1-3.

Figure 1. Map showing the location of the three study areas (Mount Hood area, Newberry Volcano, and the Breitenbush-Austin Hot Springs area) that are included in this study of hydrothermal alteration in the Pacific Northwest's Cascade Mountain Range (shaded areas)

Figure 2. Scanning electron micrograph of colorless, euhedral, trapezohedral, analcime crystals that cement early Miocene volcanic breccia fragments in the Breitenbush Hot Springs area. Tiny fibrous crystals are mordenite.

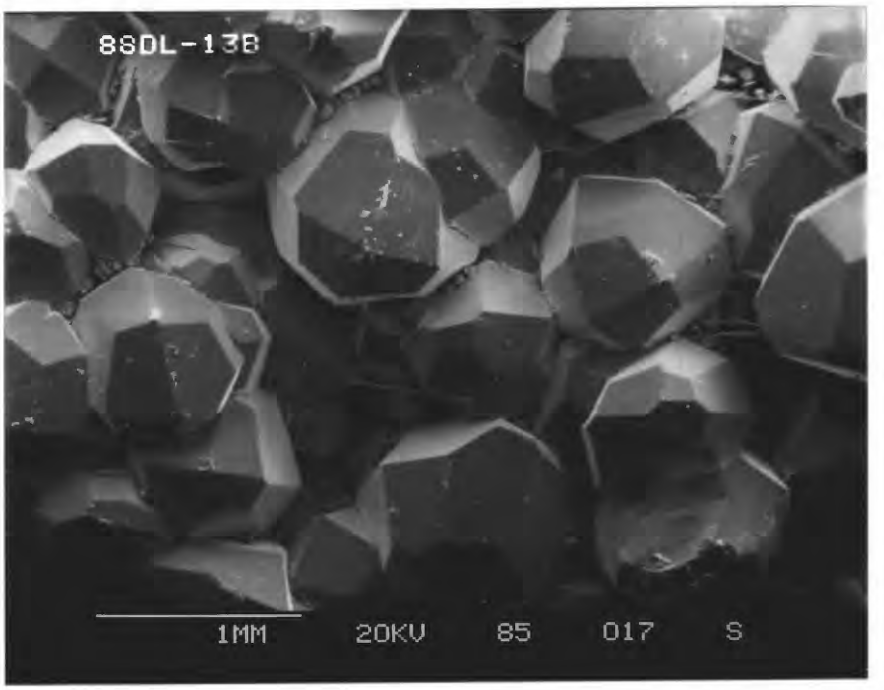

Figure 3. Ca+Mg—Na—K+Ba+Sr ternary diagram for microprobe analyses of: (A) analcime and wairakite, (B) chabazite, and (C) dachiardite from outcrops and geothermal drill holes in the Oregon Cascades.

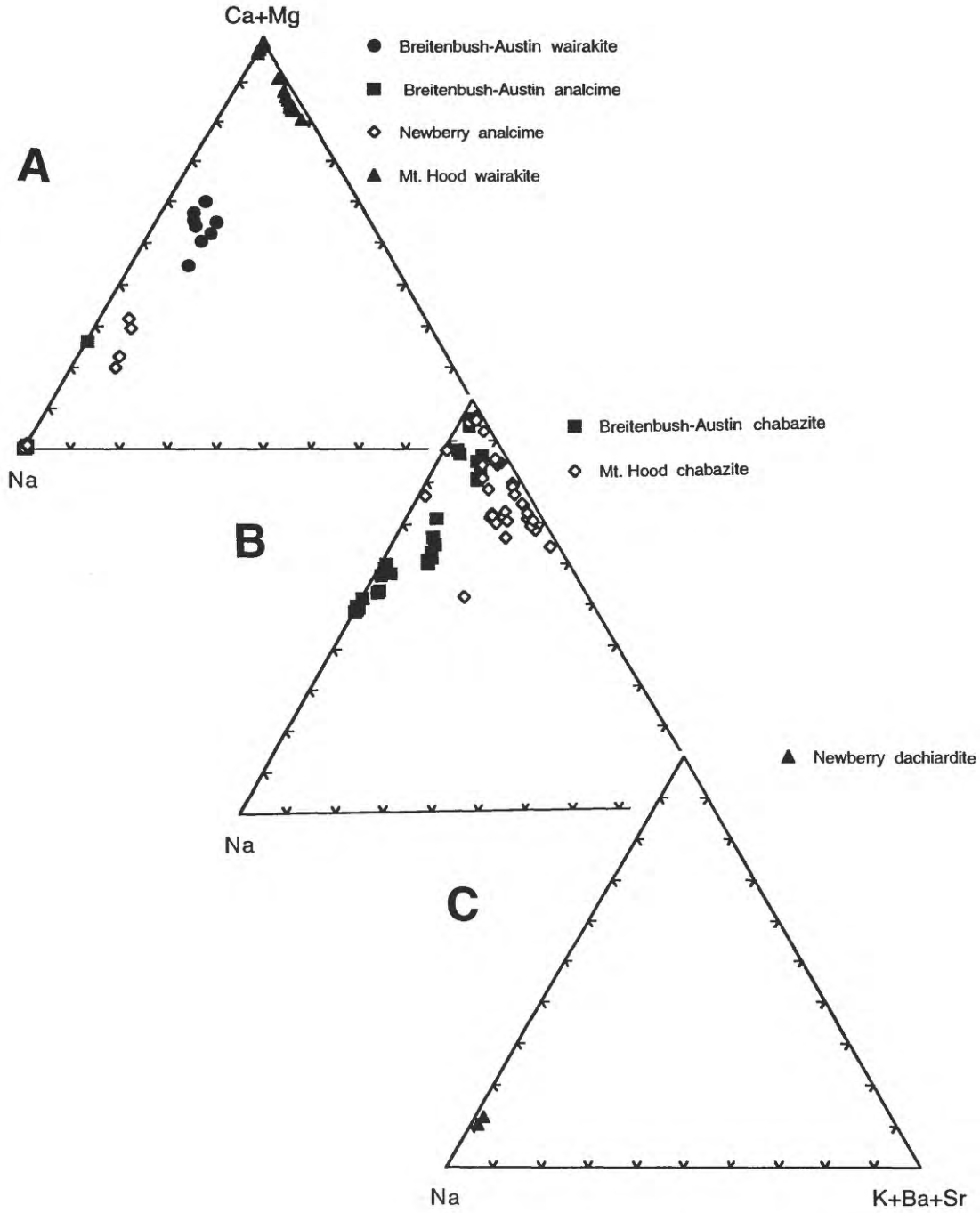

Figure 4. Scanning electron micrographs showing: (A) colorless, euhedral, pseudocubic chabazite crystals coating vesicles in Pliocene(?) andesite from an outcrop near Austin Hot Springs. (B) Colorless, lens-shaped (phacolitic) chabazite crystals deposited on faujasite coating a veinlet in basaltic sandstone from 308.9 m depth in USGS-N2 Newberry drill hole. Distance between white tic marks at bottom of micrograph is 100 μm.

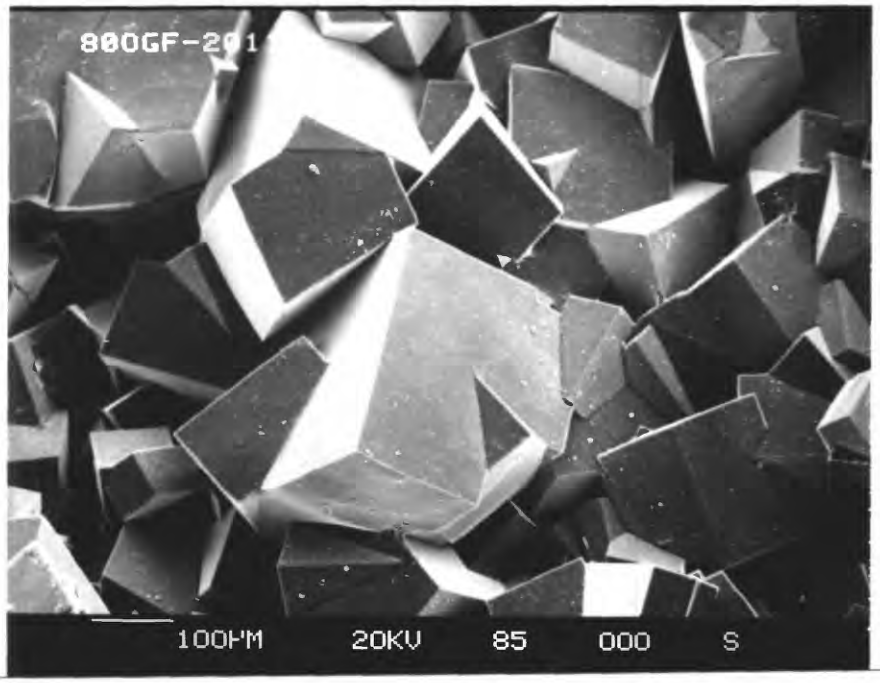


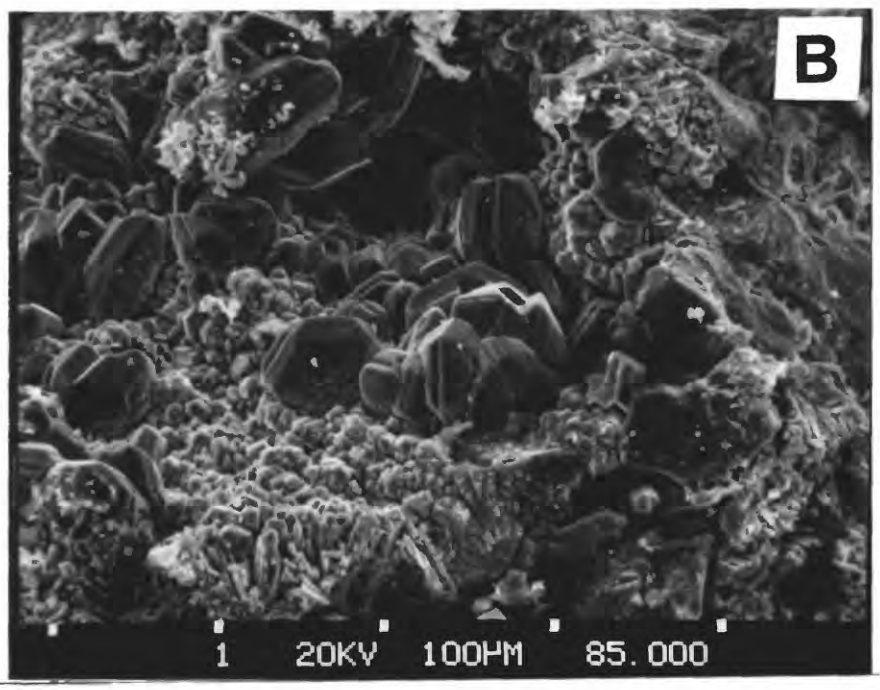

Figure 5. Ca+Mg—Na—K+Ba+Sr ternary diagram for microprobe analyses of: (A) epistilbite, (B) erionite, (C) faujasite, and (D) ferrierite from the Oregon Cascades.

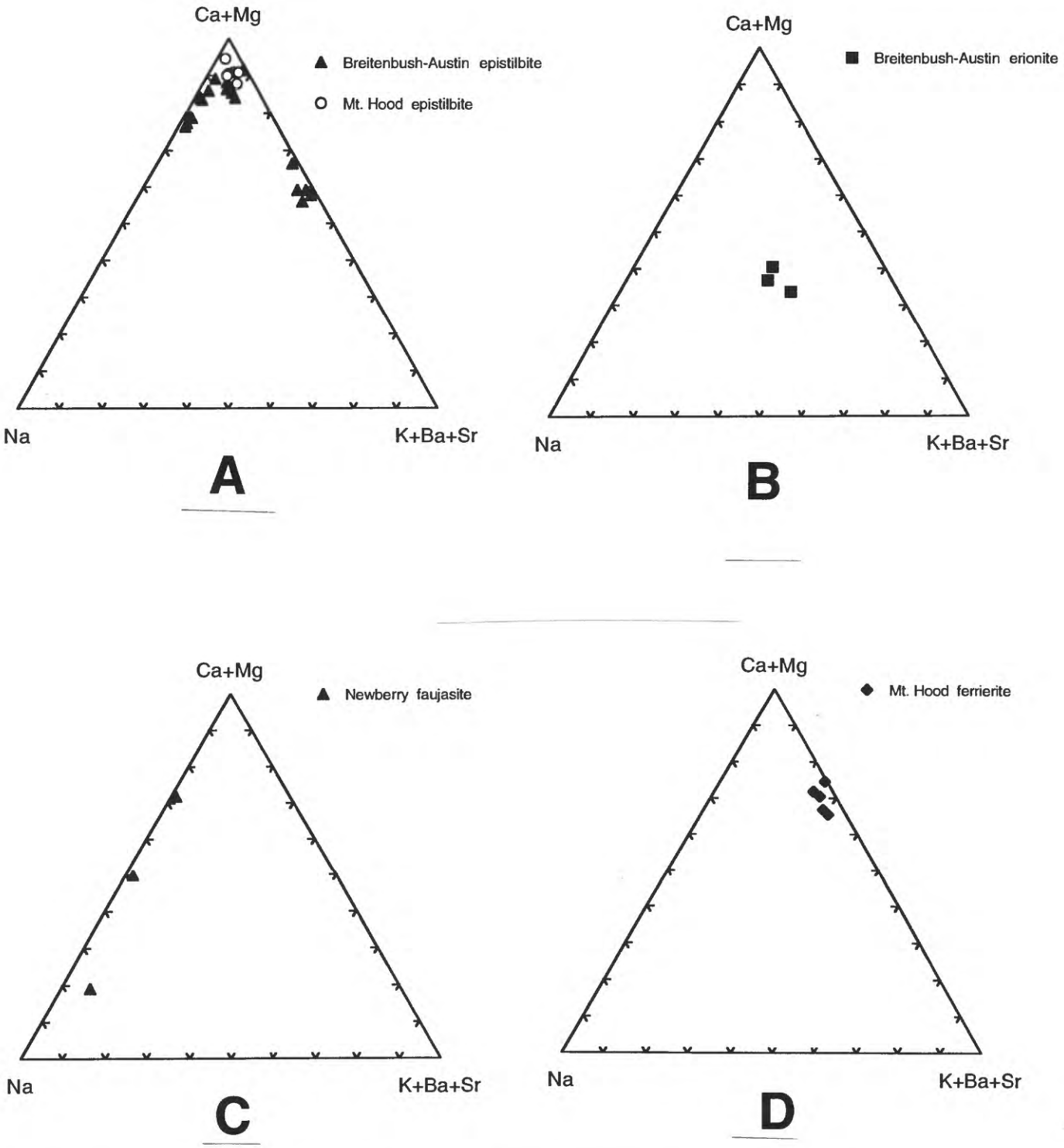

Figure 6. Scanning electron micrograph showing hexagonal bundles of fibrous erionite and later blocky heulandite crystals filling vesicles in basaltic andesite breccia fragments from 887 m depth in the CTGH-1 drill hole

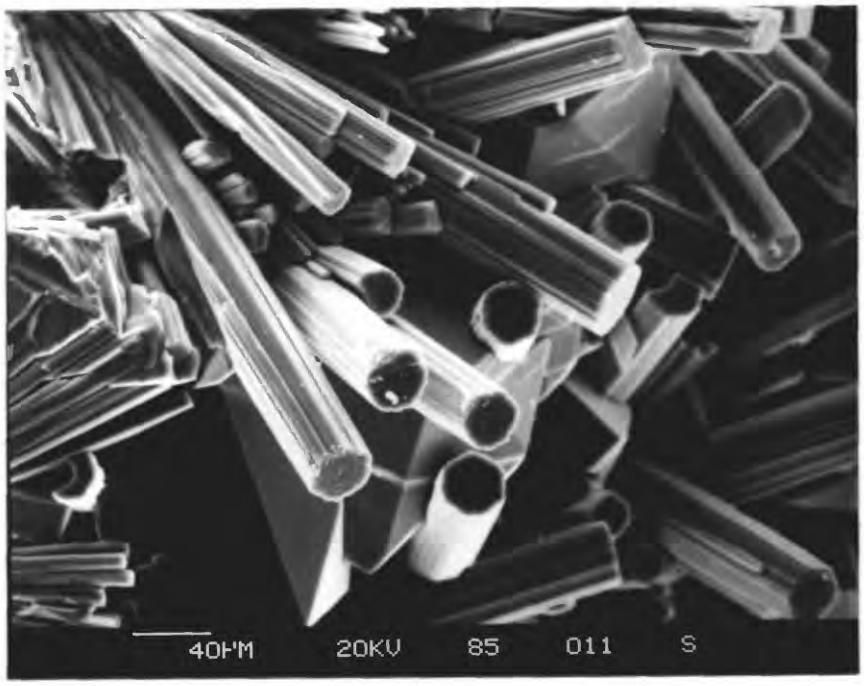

Figure 7. Scanning electron micrograph of fractured and flaking faujasite crystals filling a veinlet in basaltic sandstone from 308.9 m depth in the USGS-N2 drill hole at Newberry Volcano. Distance between white tic marks at bottom of micrograph is 10 μm.

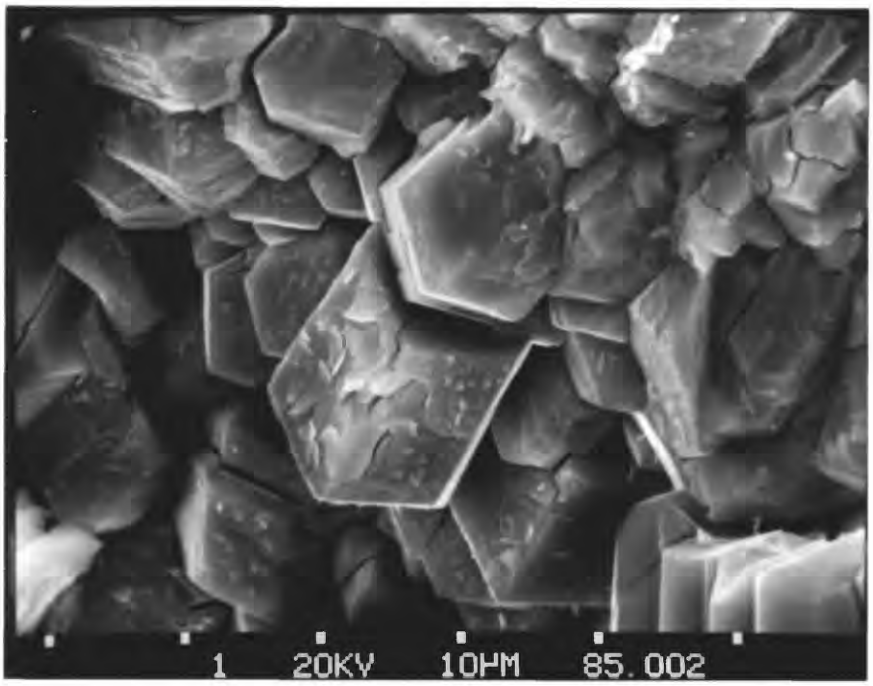

Figure 8. Scanning electron micrograph showing bladed ferrierite crystals from an outcrop near Mount Hood.

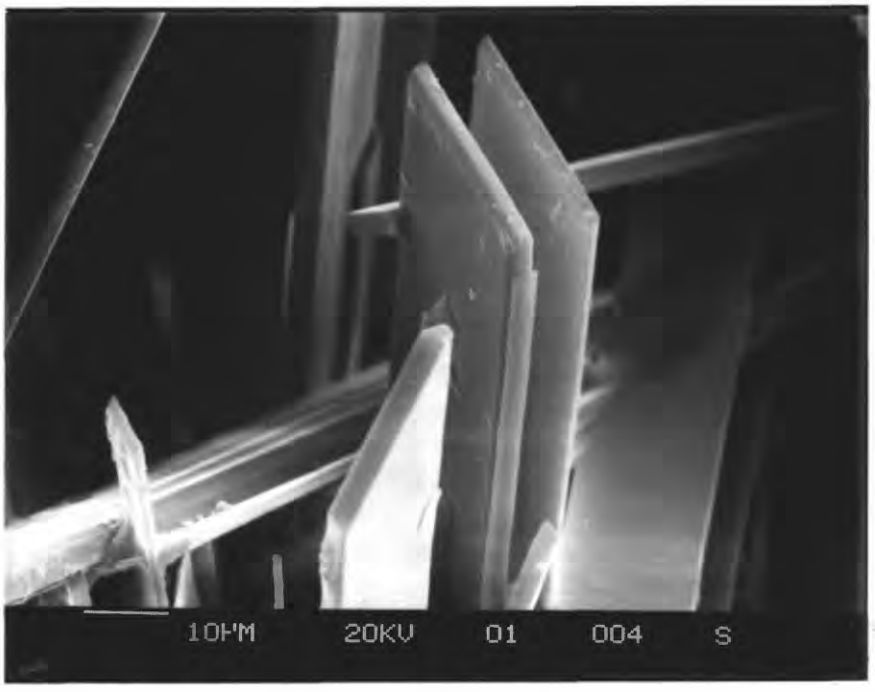

Figure 9. Scanning electron micrograph of pseudotetragonal gismondine crystals in association with penetration twinned chabazite crystals (lower left) filling vesicles in basaltic rock from the Oak Grove Fork of the Clackamas River.

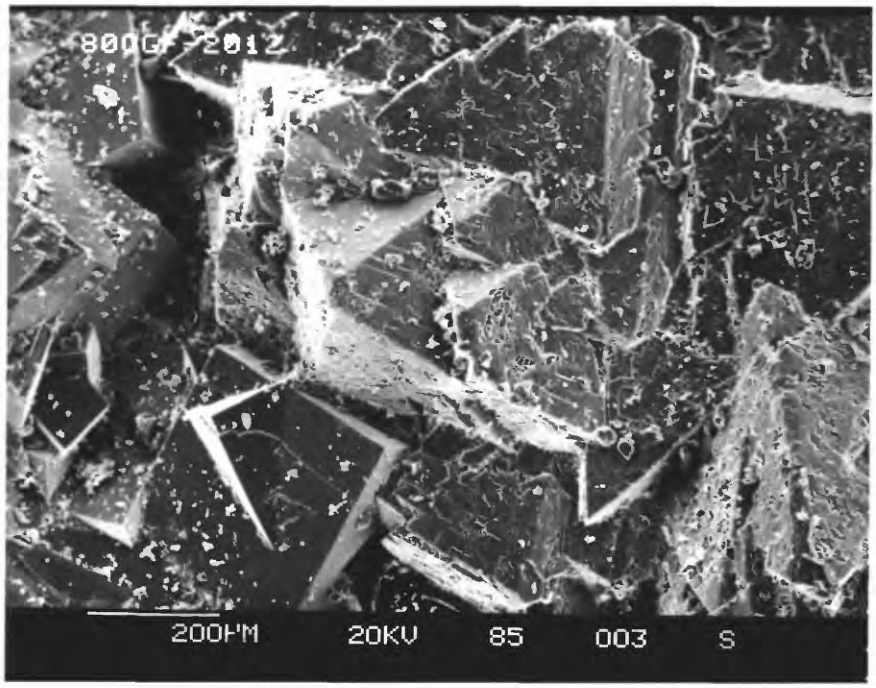

Figure 10. Scanning electron micrographs of (A) euhedral harmotome crystals from near Mount Hood; (B) radiating prisms of phillipsite crystals that fill open spaces between breccia fragments in core from 812 m depth in the CTGH-1 drill hole; and (C) prismatic wellsite crystals and later smectite that coat vesicles in basaltic andesite at 564 m depth in CTGH-1.

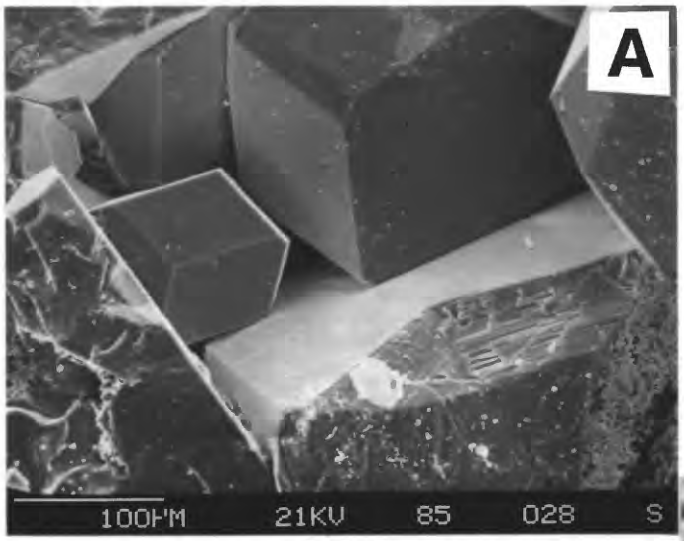


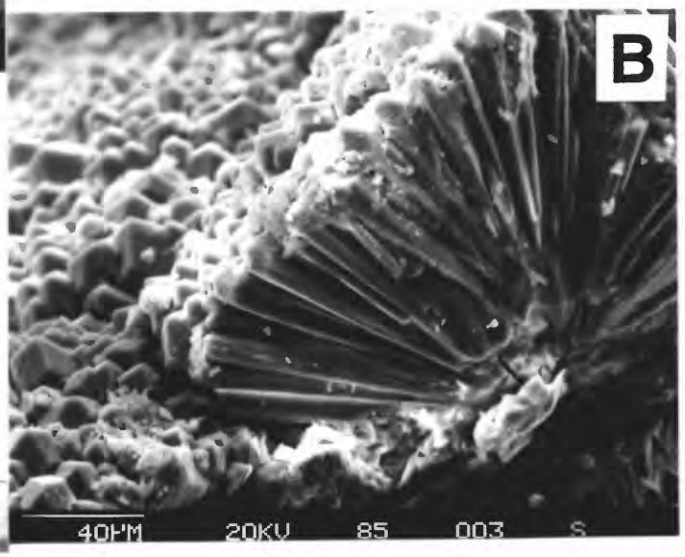


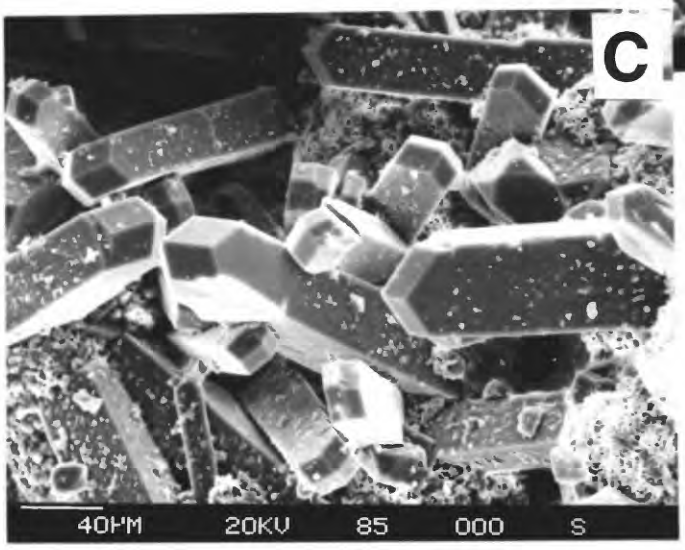

Figure 11. (A) Ba+Sr—Ca+Mg+Na—K and (B) Ca+Mg—Na—K+Ba+Sr ternary diagrams for electron microprobe analyses of harmotome, phillipsite, and wellsite from the Oregon Cascades.

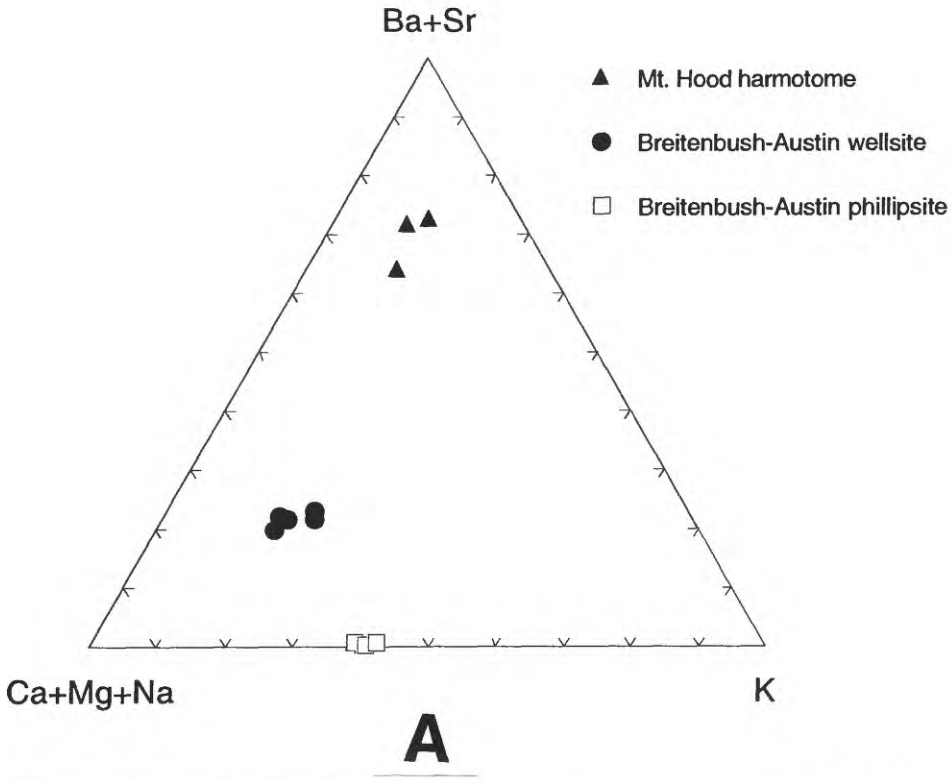


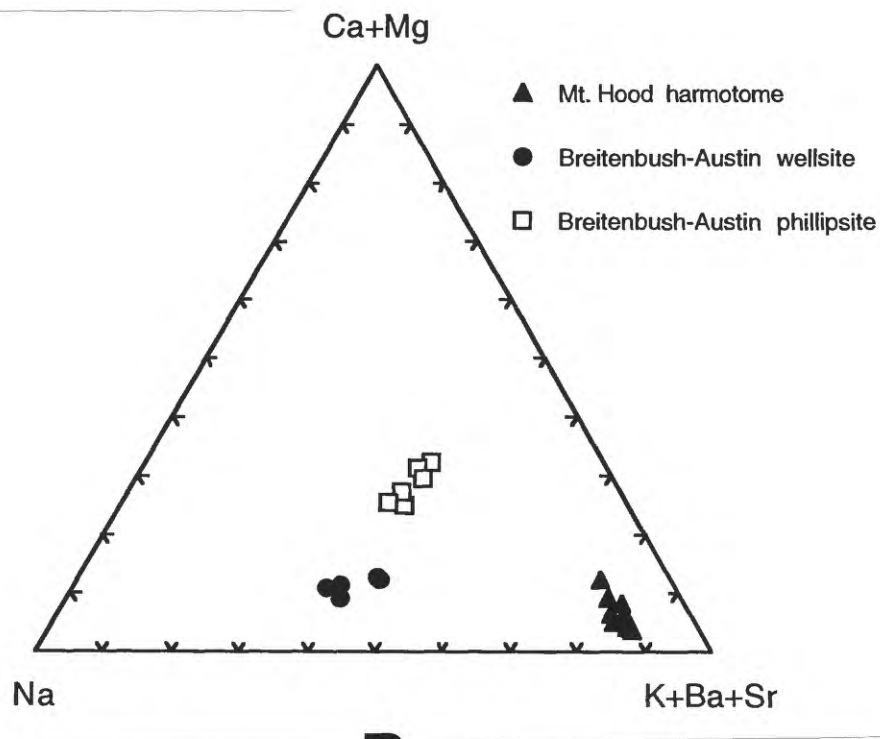

Figure 12. Vesicle fillings in a very vesicular basaltic rock outcrop from the Oak Grove Fork of the Clackamas River that contain colorless, euhedral, tabular heulandite crystals and later hemispheric cristobalite.

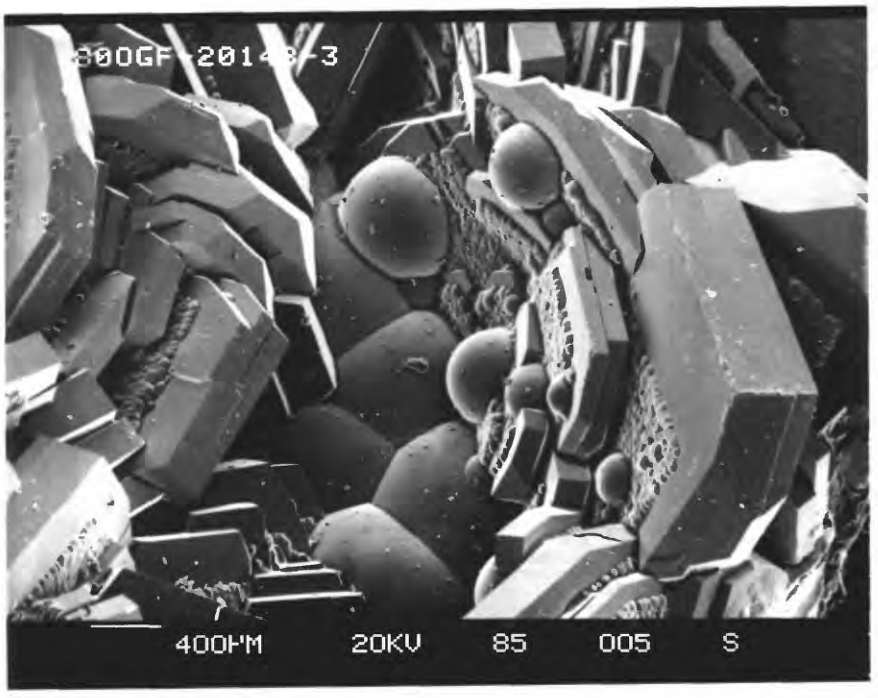

Figure 14. Scanning electron micrograph showing euhedral laumontite crystals that coat a rock fragment in drill cuttings from 1125 m depth in the Pucci geothermal drill hole located on the southern slopes of Mount Hood. Distance between white tic marks at bottom of micrograph is 30 μm.

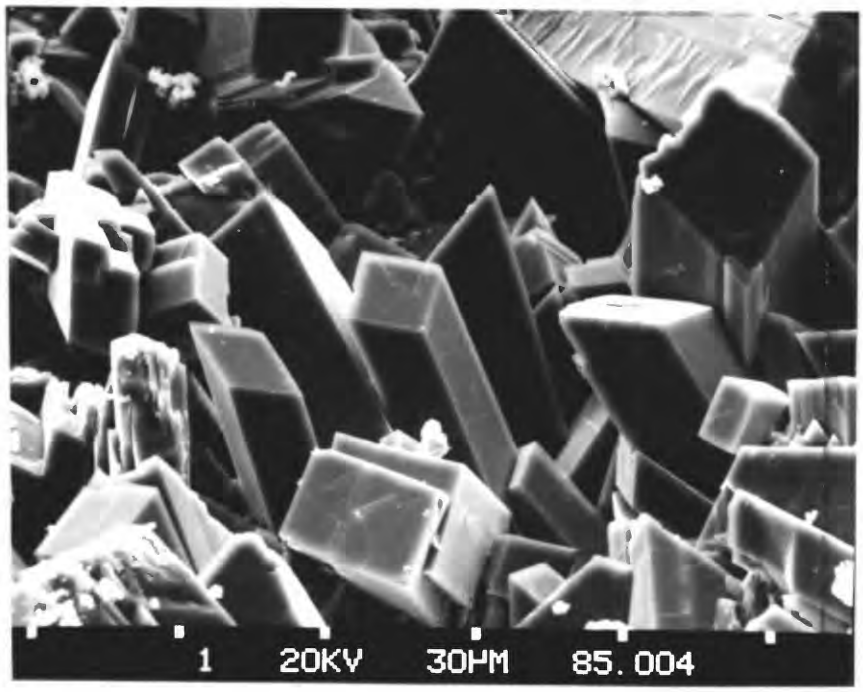

Figure 13. Ca+Mg—Na—K+Ba+Sr ternary diagram for electron microprobe analyses of heulandite-group minerals from the Oregon Cascades.

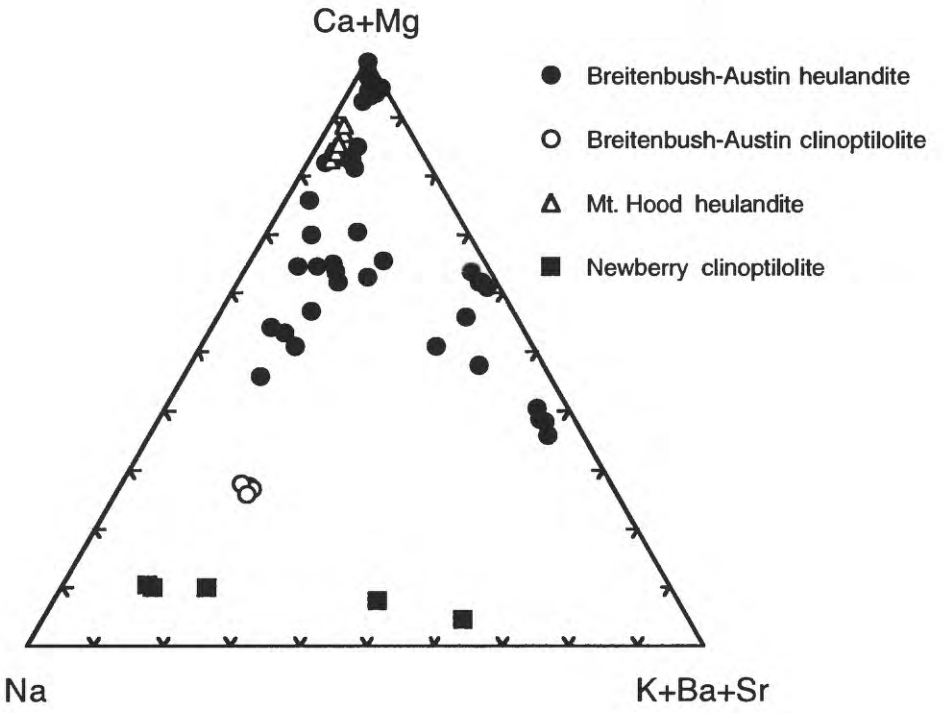

Figure 16. Scanning electron micrograph showing acicular mesolite crystals that coat fractures at 767 m depth in the CTGH-1 drill hole located near Breitenbush Hot Springs. Tabular mineral in the upper right and lower left corners of the figure is thomsonite. Both of these minerals are lightly coated by late smectite.

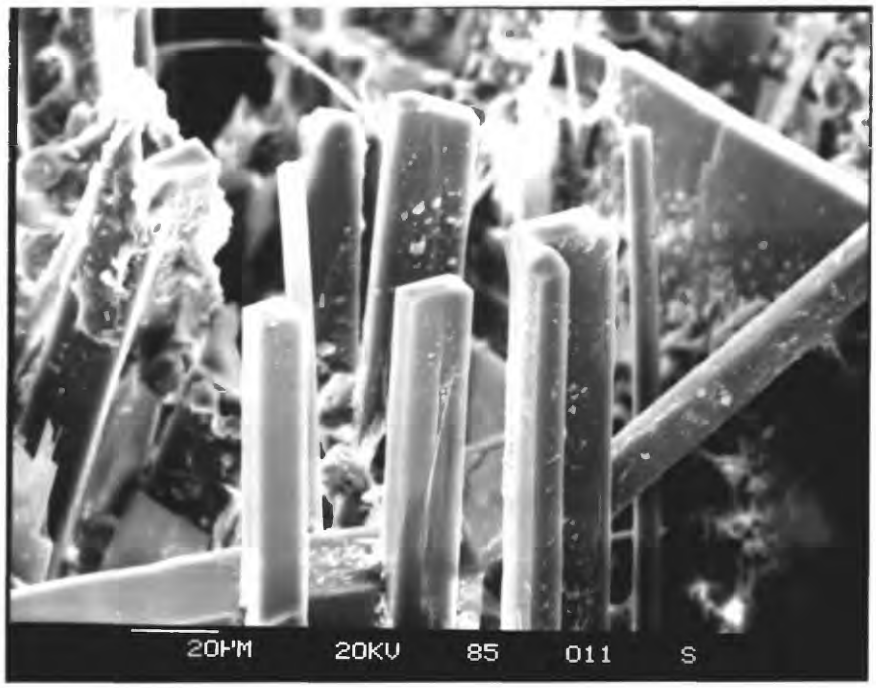

Figure 15. Ca+Mg—Na—K+Ba+Sr ternary diagram for electron microprobe analyses of: (A) laumontite, (B) mesolite, and (C) scolecite specimens collected from near Mount Hood and the Breitenbush-Austin Hot Springs areas.

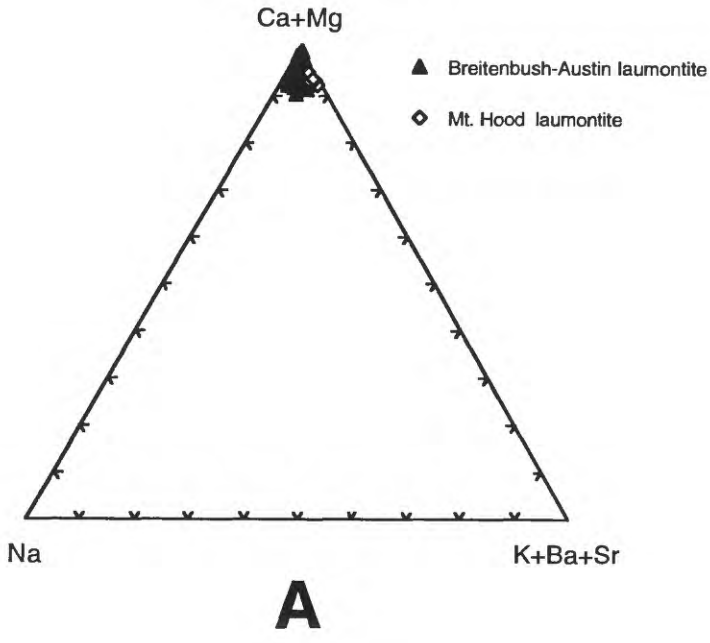


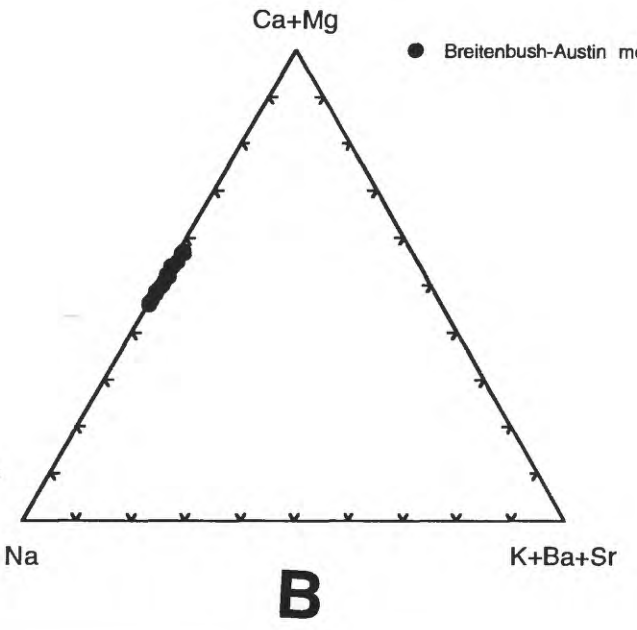


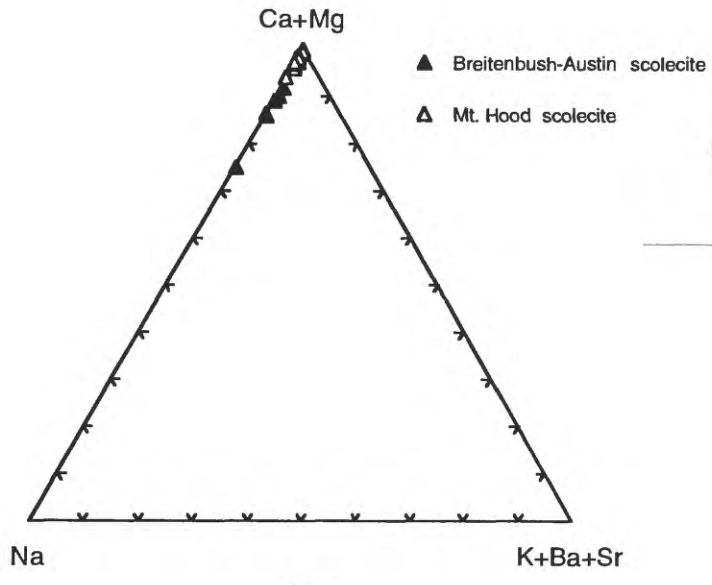

Figure 17. Scanning electron micrograph showing fibrous mordenite and earlier disk-shaped clusters of siderite coating open spaces between breccia fragments in core from 496 m depth in the USGS-N2 drill hole.

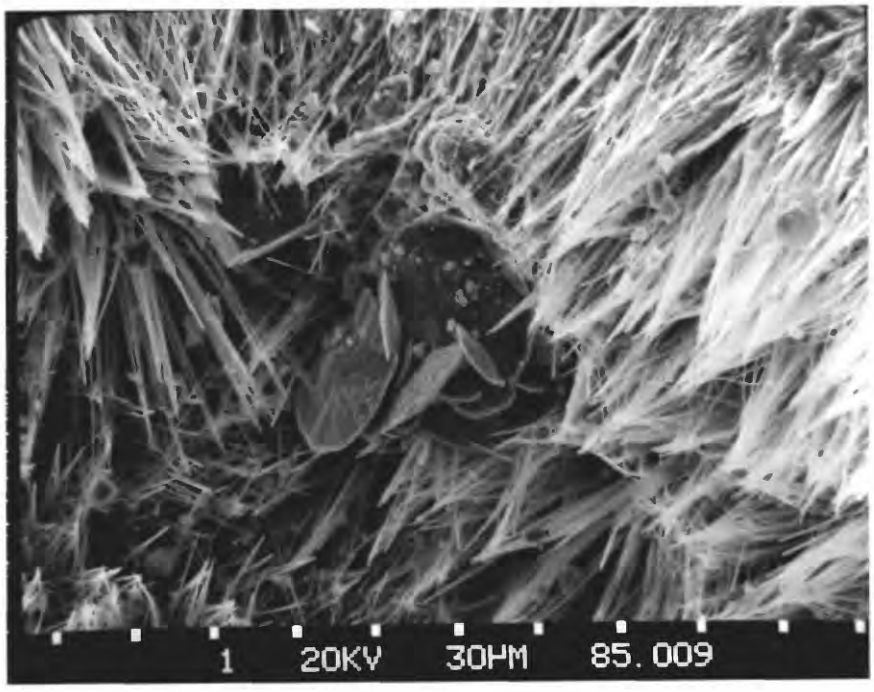

Figure 18. Scanning electron micrographs showing different morphologies for stilbite/stellerite that coats rock fragments in drill cuttings from (A) 134 m depth in the Zigzag River geothermal drill hole and (B) 1161 m depth in the Pucci drill hole. Both drill holes are located near Mount Hood (Bargar, Keith, and Beeson, 1993). Distance between white tic marks at bottom of micrograph is 100 μm.

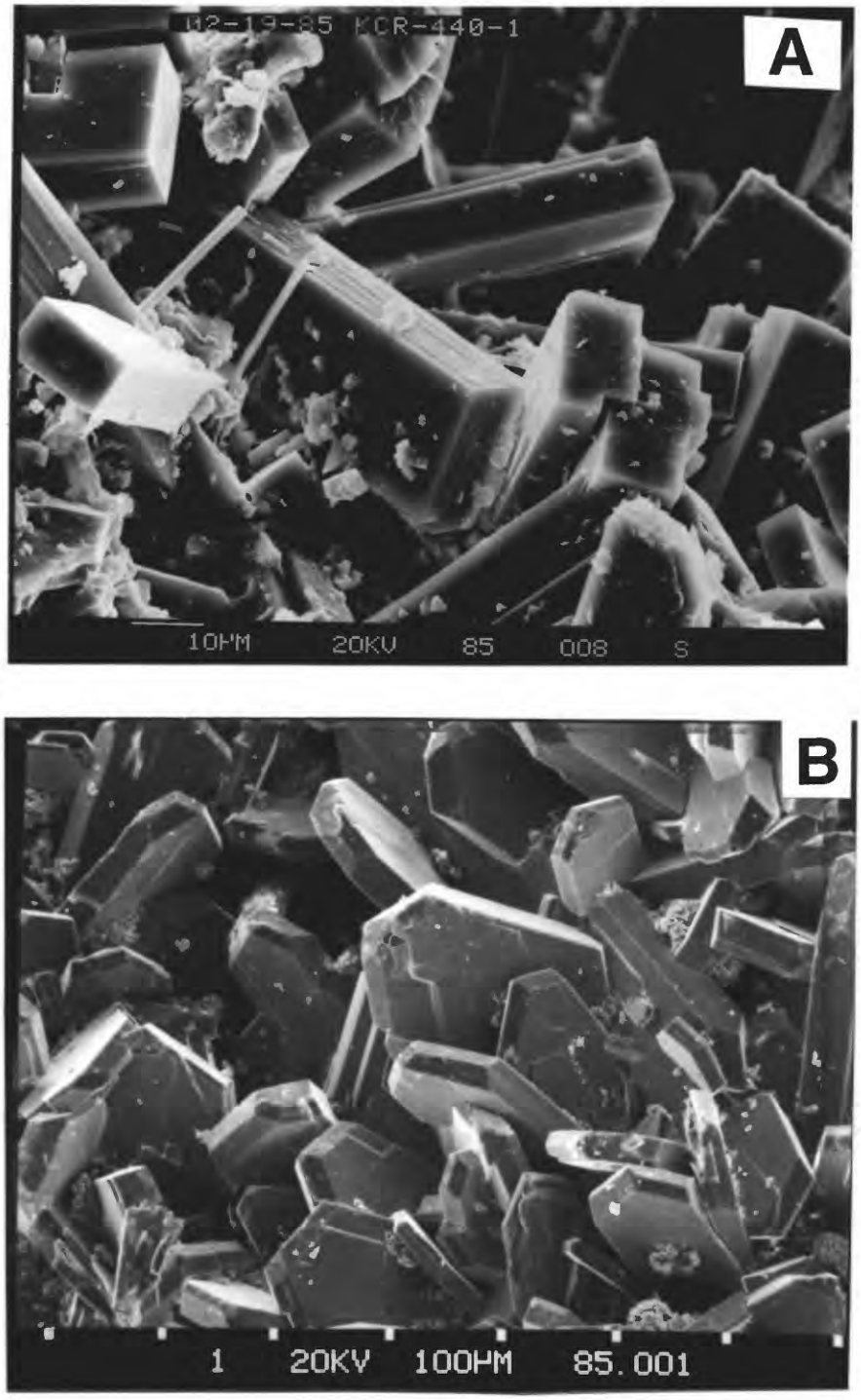

Figure 19. Ca+Mg—Na—K+Ba+Sr ternary diagrams for electron microprobe analyses of (A) stilbite/stellerite, (B) thomsonite, and (C) yugawaralite from the Breitenbush-Austin Hot Springs and Mount Hood areas .

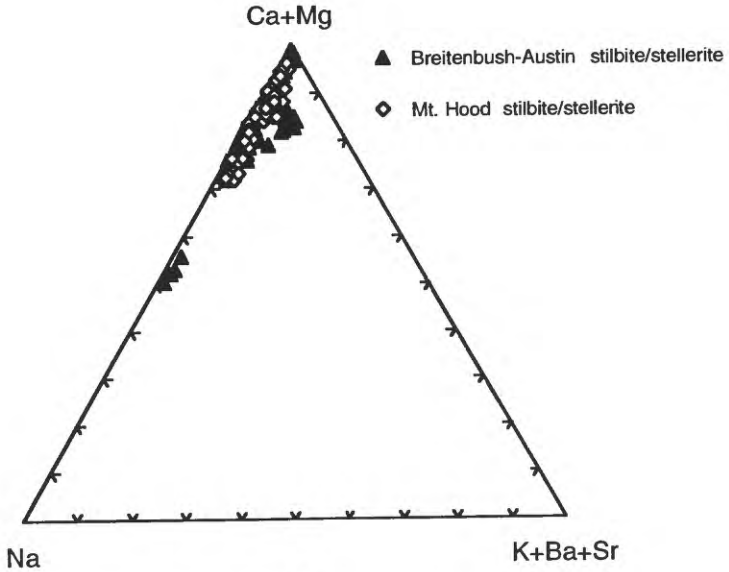


A

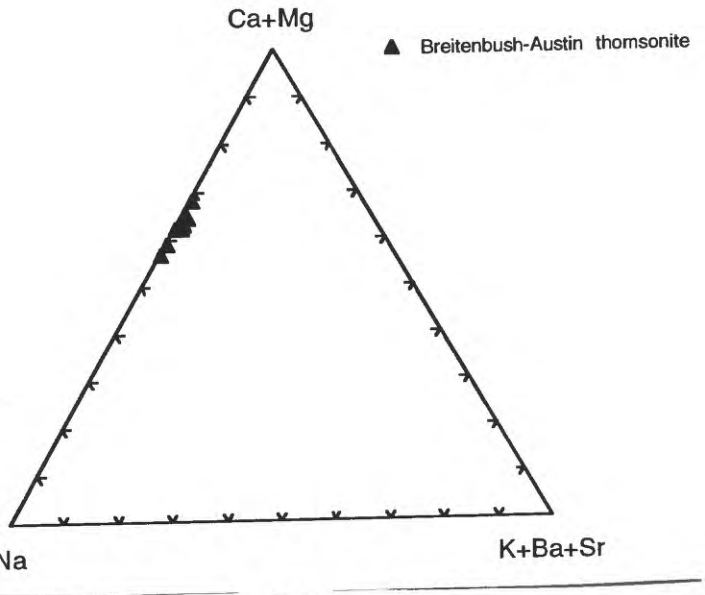


B

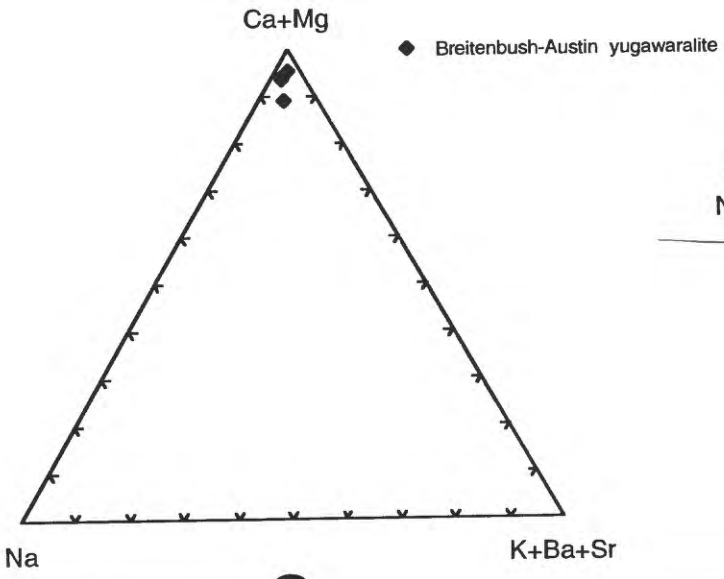


C

Figure 20. Scanning electron micrograph showing bladed thomsonite and acicular scolecite that fill fractures in a basalt outcrop in the Breitenbush-Austin Hot Springs area.

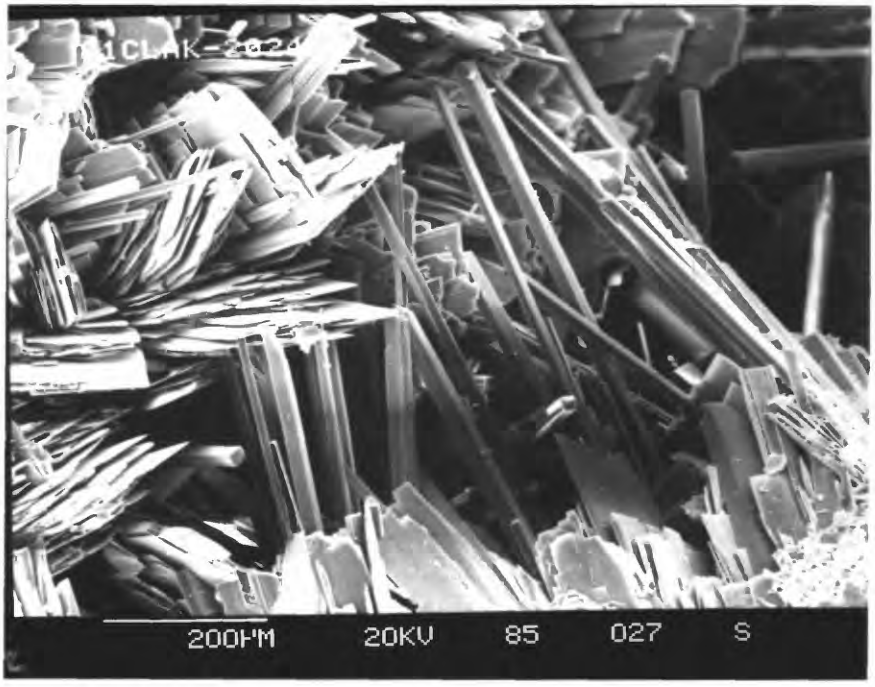

Figure 21. Scanning electron micrograph of blocky adularia and earlier tiny quartz crystals from an outcrop in the Breitenbush-Austin Hot Springs area.

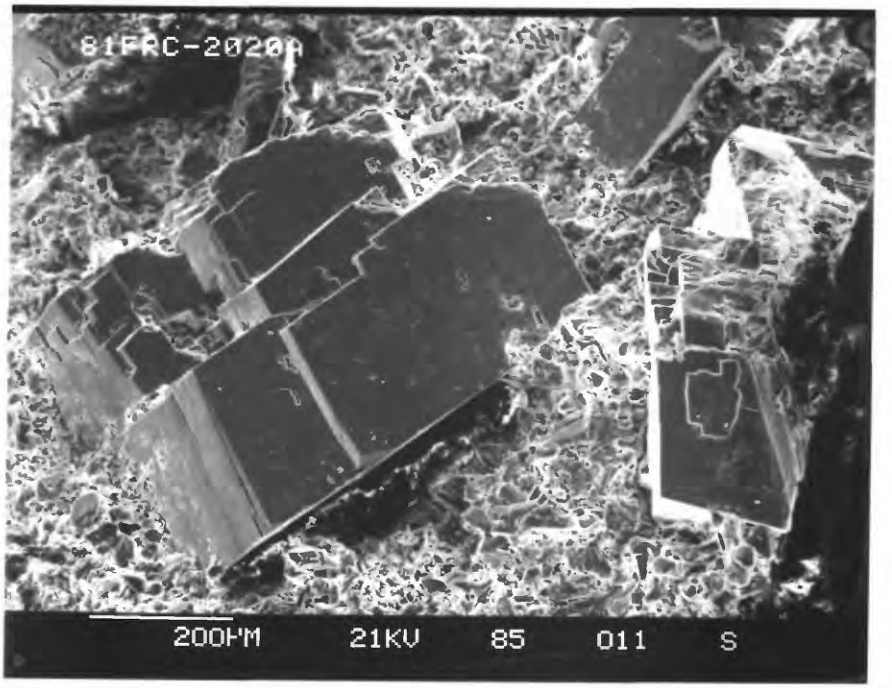

Figure 22. Scanning electron micrograph of colorless, blocky to pyramid-shaped, euhedral, apophyllite crystals that fill vesicles in a basaltic outcrop located about 9 kilometers ENE of Mt. Jefferson.

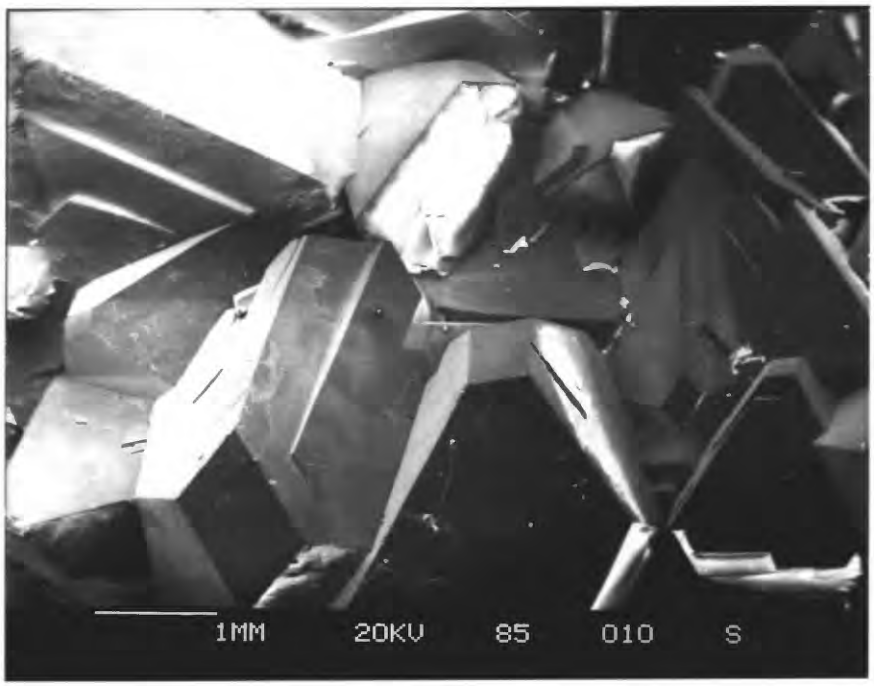

Figure 23. Scanning electron micrograph showing a rosette of well-crystallized chlorite fracture filling from near the old Quartzville mining region.

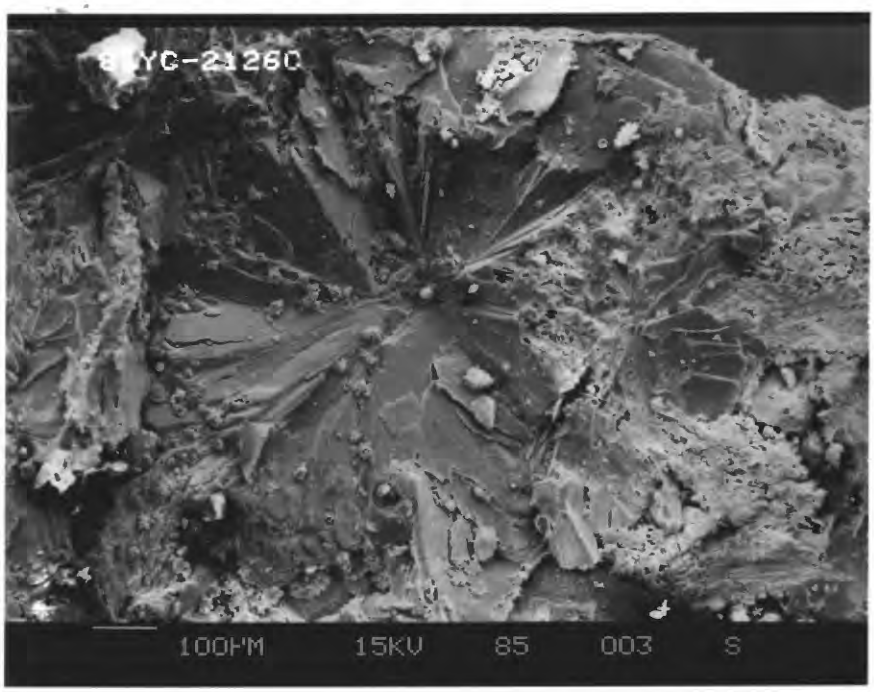

Figure 25. Scanning electron micrograph of wedge-shaped clusters of rhombic dolomite crystals from the same area as Figure 24.

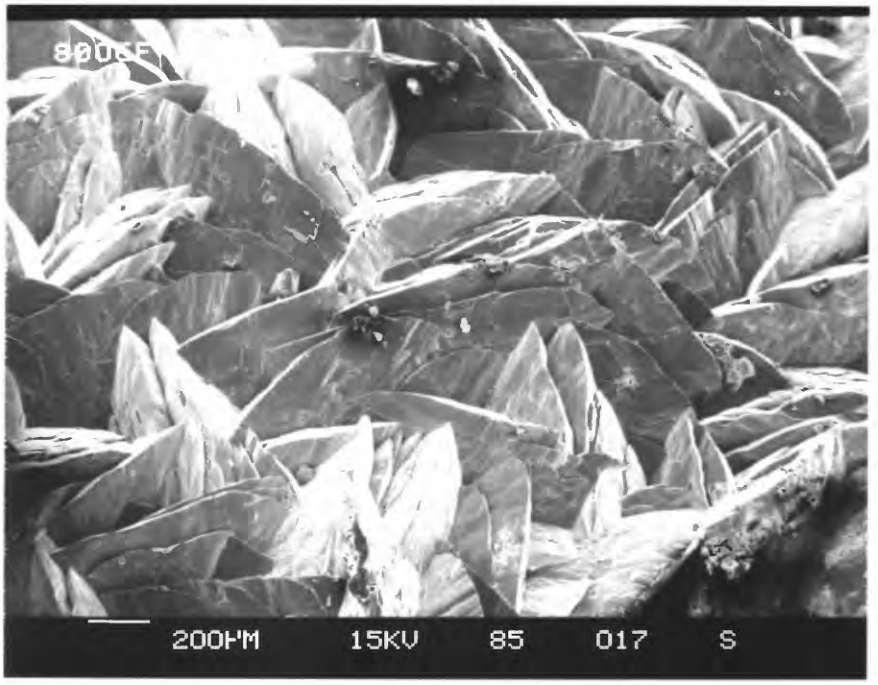

Figure 26. Scanning electron micrograph of randomly oriented, euhedral to subhedral, acicular epidote crystals from a late Tertiary intrusive in the Breitenbush-Austin Hot Springs area.

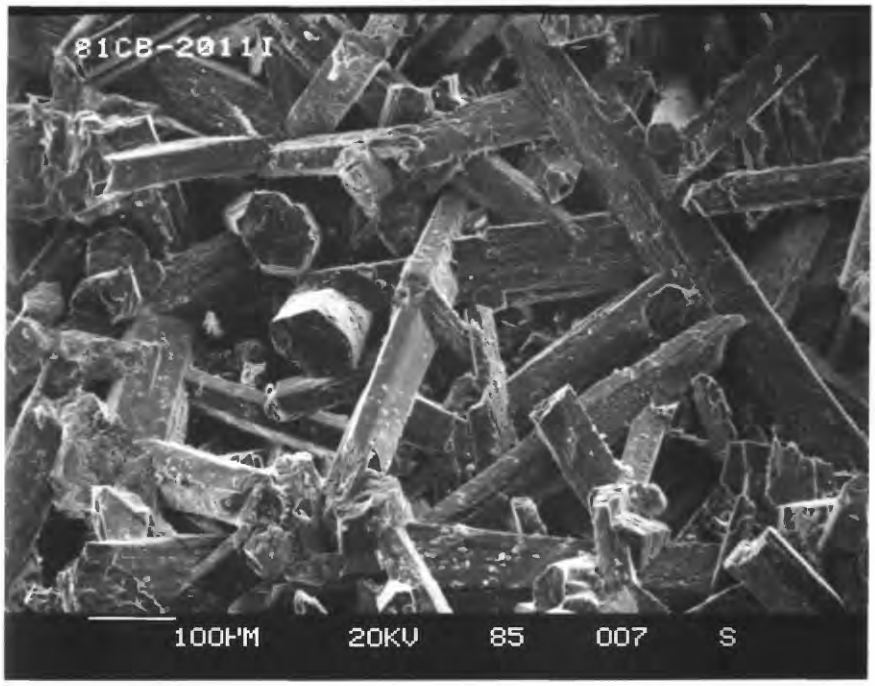

Figure 27. Scanning electron micrograph showing subhedral to euhedral garnet crystals collected near a small late Tertiary intrusive in the Breitenbush-Austin Hot Springs area.

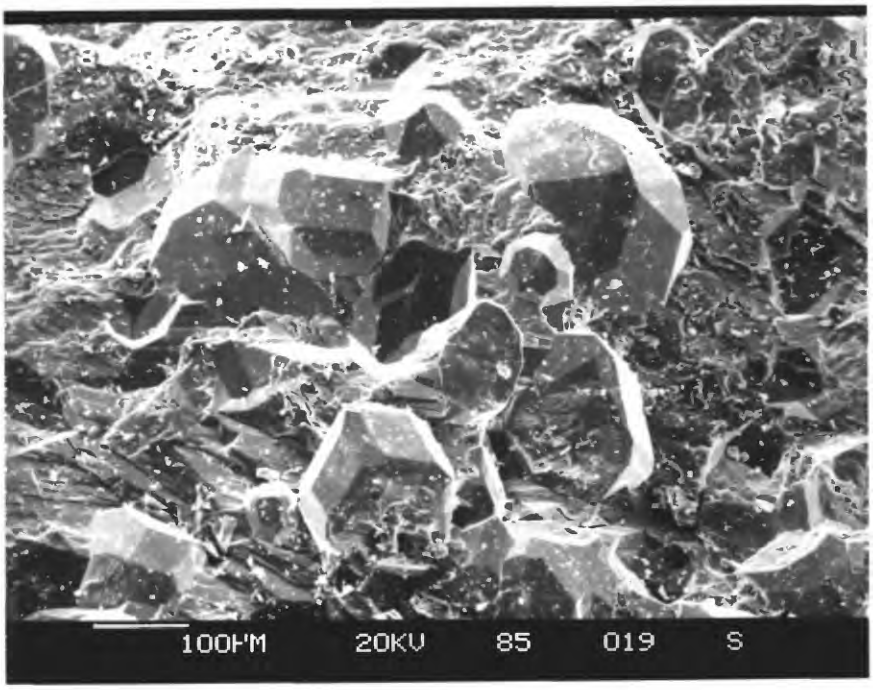

Figure 24. Scanning electron micrograph showing an open space filling of cinnabar and earlier quartz from an abandoned mining area on the banks of the Oak Grove Fork of the Clackamas River.

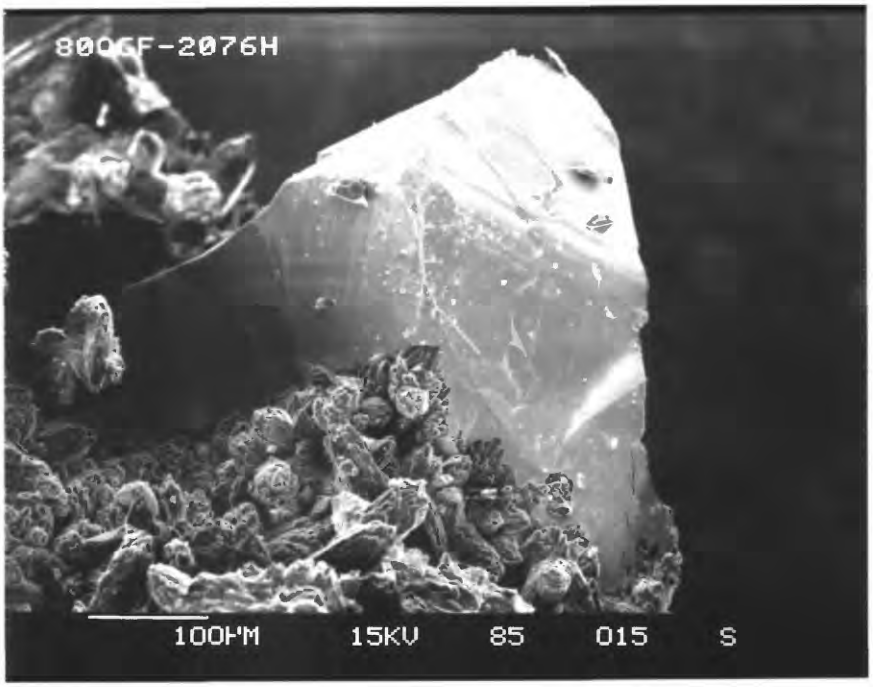

Figure 28. Scanning electron micrograph showing rosettes of smectite crystals coating a fracture surface of a late Tertiary volcanic rock in the Breitenbush-Austin Hot Springs area.

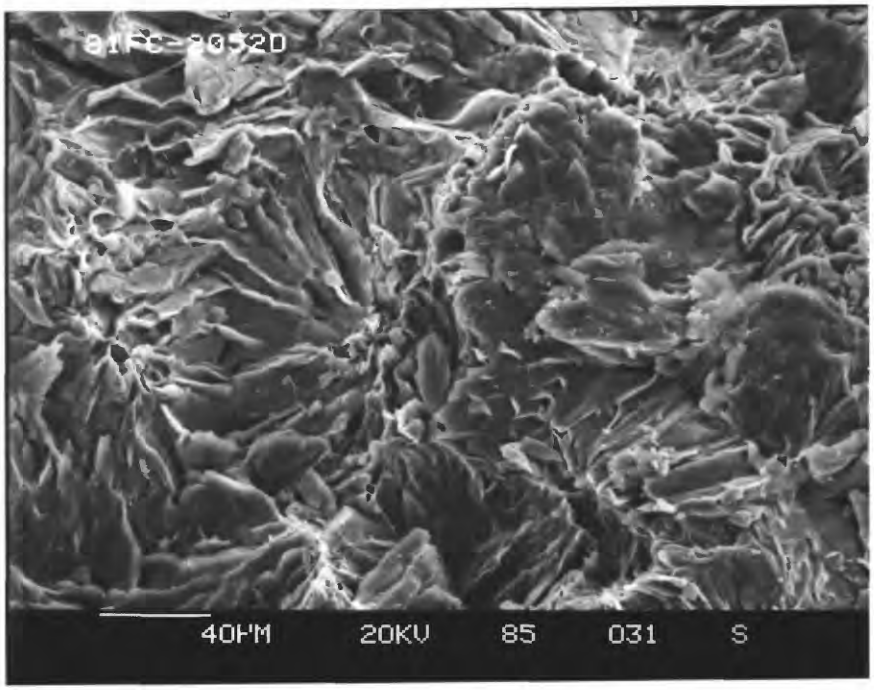

Figure 29. Depth versus homogenization temperatures for fluid inclusions in minerals (only calcite, anhydrite, and primary quartz are believed to be authigenic) from the SUNEDCO 58-28 drill hole. Dotted curve SBPC is a theoretical reference boiling point curve for pure water drawn to the ground surface. Solid curve shows a measured-temperature profile using data in Blackwell and others (1986); the continuing dashed line is an estimate of temperatures in the lower part of the drill hole based on a bottom-hole temperature of ~141°C (A.F. Waibel, unpublished data, 1982). Individual homogenization temperature measurements are plotted at 5°C intervals as histograms with sample depth as a baseline. Baseline at 1,470 m depth is stepped-down to avoid crowding above data.

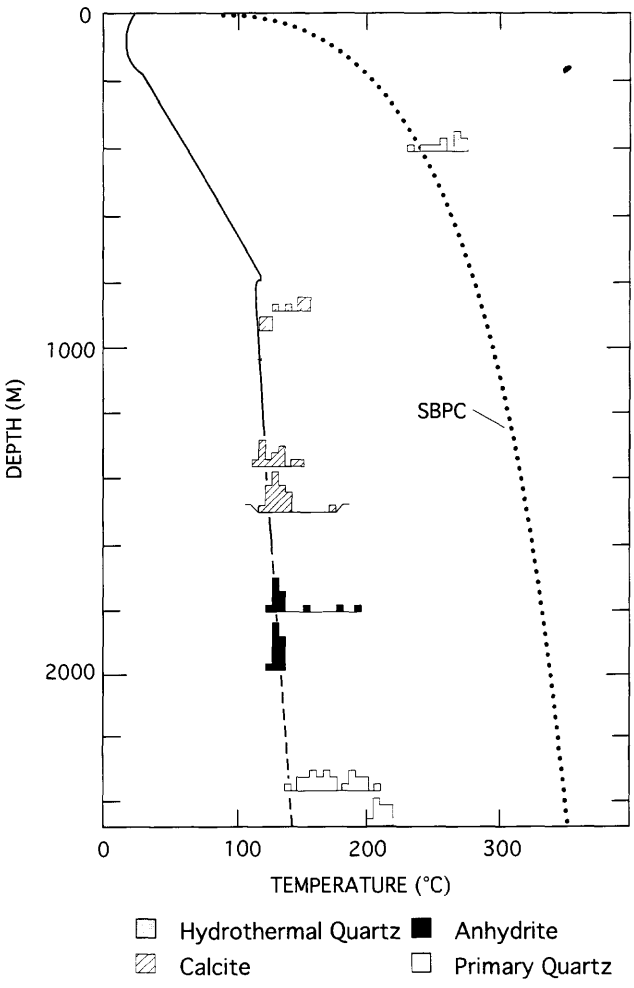

Figure 30. Histograms of homogenization temperature (Th) measurements for fluid inclusions in (A) authigenic minerals from the SUNEDCO 58-28 drill hole, (B) hydrothermal quartz and calcite from outcrop specimens elsewhere in the Breitenbush-Austin Hot Springs area, and (C) hydrothermal quartz from the intrusive at Detroit Lake.

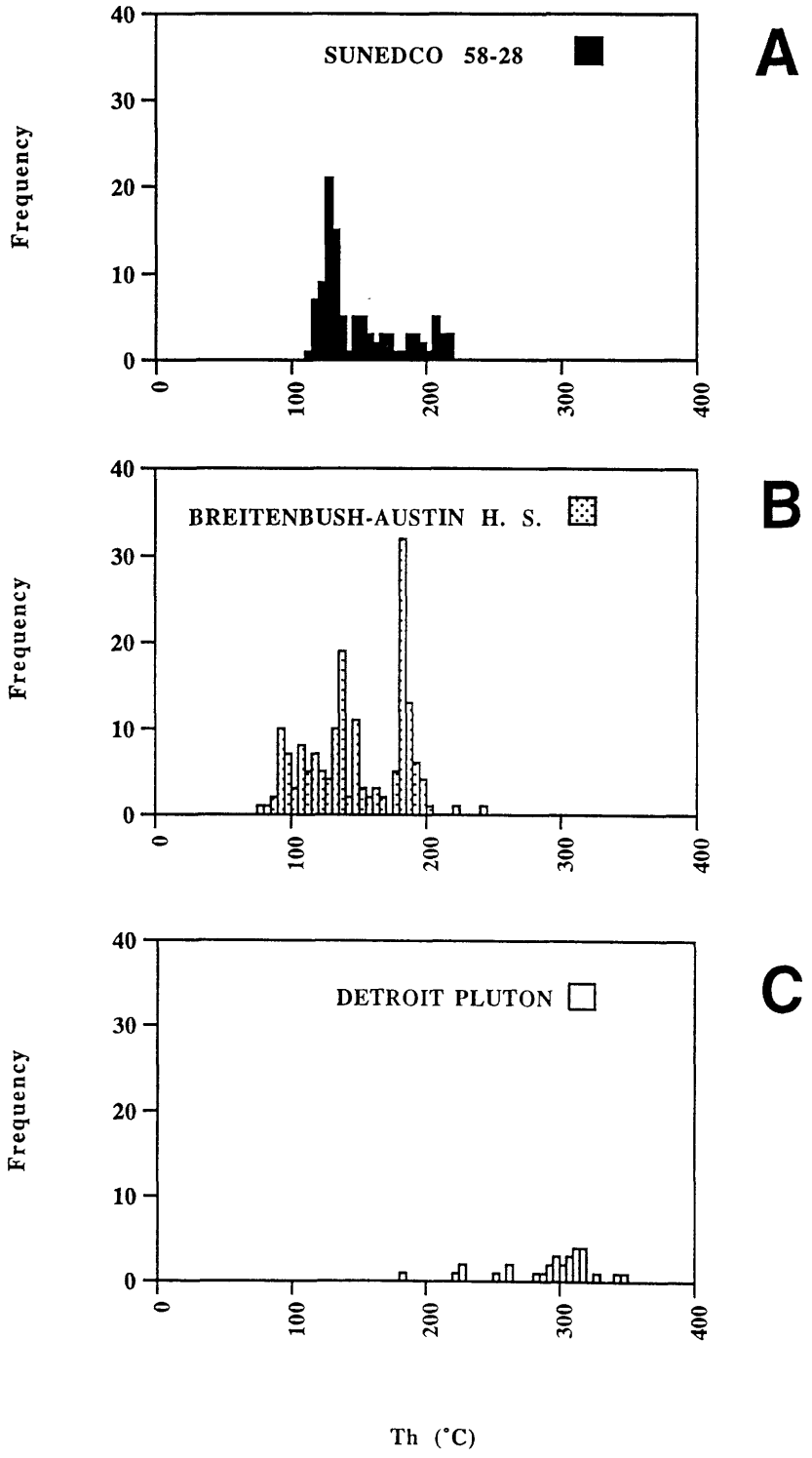

Figure 31. Map of the Breitenbush-Austin Hot Springs area showing the location of geothermal drill holes SUNEDCO 58-28 and CTGH-1 as well as locations of samples utilized for fluid inclusion studies.

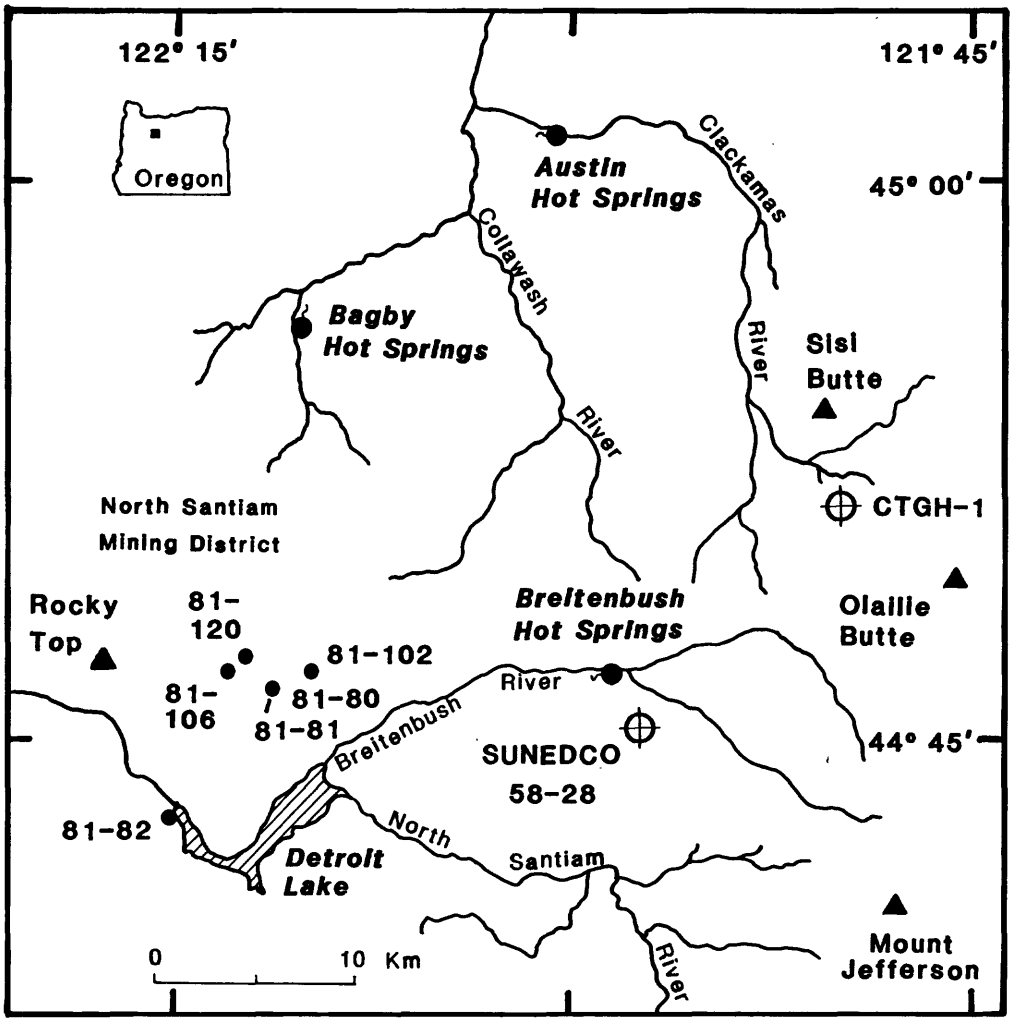

Table 1. Electron microprobe analyses of actinolite/tremolite (total iron reported as FeO).

| Sample no. | 81CB-2006B | | | | |
|---|---|---|---|---|---|
| Analysis no. | 1 | 2 | 3 | 4 | 5 |
| | Major-element chemical analyses (weight percent oxides) | | | | |
| $SiO_2$ | 50.96 | 51.01 | 49.96 | 49.26 | 50.28 |
| $Al_2O_3$ | 2.72 | 2.49 | 3.61 | 3.40 | 3.23 |
| FeO | 14.65 | 14.51 | 16.60 | 17.66 | 16.13 |
| MgO | 13.50 | 13.97 | 12.17 | 11.75 | 13.11 |
| CaO | 11.44 | 11.18 | 10.74 | 11.24 | 10.70 |
| $Na_2O$ | 0.26 | 0.25 | 0.37 | 0.30 | 0.29 |
| $K_2O$ | 0.07 | 0.08 | 0.09 | 0.07 | 0.09 |
| MnO | 0.38 | 0.32 | 0.56 | 0.53 | 0.54 |
| SrO | 0.03 | 0.02 | 0.00 | 0.04 | 0.06 |
| BaO | 0.06 | 0.00 | 0.16 | 0.00 | 0.09 |
| Total | 94.07 | 93.83 | 94.26 | 94.25 | 94.52 |
| | Number of atoms on the basis of 24 oxygens | | | | |
| Si | 8.05 | 8.06 | 7.95 | 7.90 | 7.96 |
| Al | 0.00 | 0.00 | 0.05 | 0.10 | 0.04 |
| Al | 0.51 | 0.46 | 0.63 | 0.54 | 0.56 |
| Fe | 1.93 | 1.92 | 2.21 | 2.37 | 2.14 |
| Mg | 3.18 | 3.29 | 2.89 | 2.81 | 3.09 |
| Ca | 1.94 | 1.89 | 1.83 | 1.93 | 1.82 |
| Na | 0.08 | 0.08 | 0.11 | 0.09 | 0.09 |
| K | 0.01 | 0.02 | 0.02 | 0.01 | 0.02 |
| Mn | 0.05 | 0.04 | 0.08 | 0.07 | 0.07 |
| Sr | 0.00 | 0.00 | 0.00 | 0.00 | 0.01 |
| Ba | 0.00 | 0.00 | 0.00 | 0.00 | 0.01 |
| 100Mg/(Mg+Fe+Mn) | 61.63 | 62.67 | 55.79 | 53.52 | 58.30 |

| Sample no. | 81 CB-2038E | | | | |
|---|---|---|---|---|---|
| Analysis no. | 1 | 2 | 3 | 4 | 5 |
| | Major-element chemical analyses (weight percent oxides) | | | | |
| $SiO_2$ | 53.62 | 55.40 | 54.99 | 53.70 | 55.29 |
| $Al_2O_3$ | 1.72 | 0.73 | 1.44 | 1.19 | 0.98 |
| FeO | 16.53 | 13.00 | 12.28 | 8.71 | 12.74 |
| MgO | 12.39 | 15.27 | 15.35 | 14.81 | 15.96 |
| CaO | 12.17 | 12.51 | 11.23 | 16.92 | 12.10 |
| $Na_2O$ | 0.17 | 0.07 | 0.10 | 0.16 | 0.10 |
| $K_2O$ | 0.09 | 0.02 | 0.05 | 0.03 | 0.04 |
| MnO | 0.78 | 0.80 | 0.86 | 0.41 | 0.90 |
| SrO | 0.04 | 0.11 | 0.05 | 0.02 | 0.09 |
| BaO | 0.02 | 0.00 | 0.08 | 0.00 | 0.00 |
| Total | 97.53 | 97.91 | 96.43 | 95.95 | 98.20 |
| | Number of atoms on the basis of 24 oxygens | | | | |
| Si | 8.22 | 8.31 | 8.32 | 8.18 | 8.26 |
| Al | 0.00 | 0.00 | 0.00 | 0.00 | 0.00 |
| Al | 0.31 | 0.13 | 0.26 | 0.21 | 0.17 |
| Fe | 2.11 | 1.63 | 1.55 | 1.11 | 1.59 |
| Mg | 2.83 | 3.42 | 3.46 | 3.36 | 3.55 |
| Ca | 2.00 | 2.01 | 1.82 | 2.76 | 1.94 |
| Na | 0.05 | 0.02 | 0.03 | 0.05 | 0.03 |
| K | 0.02 | 0.00 | 0.01 | 0.01 | 0.01 |
| Mn | 0.10 | 0.10 | 0.11 | 0.05 | 0.11 |
| Sr | 0.00 | 0.01 | 0.00 | 0.00 | 0.01 |
| Ba | 0.00 | 0.00 | 0.00 | 0.00 | 0.00 |
| 100Mg/(Mg+Fe+Mn) | 56.15 | 66.40 | 67.58 | 74.34 | 67.61 |

Table 1. continued.

| Sample no. | 81 CB-2038E | | | | |
|---|---|---|---|---|---|
| Analysis no. | 1 | 2 | 3 | 4 | 5 |
| | Major-element chemical analyses (weight percent oxides) | | | | |
| $SiO_2$ | 53.62 | 55.40 | 54.99 | 53.70 | 55.29 |
| $Al_2O_3$ | 1.72 | 0.73 | 1.44 | 1.19 | 0.98 |
| FeO | 16.53 | 13.00 | 12.28 | 8.71 | 12.74 |
| MgO | 12.39 | 15.27 | 15.35 | 14.81 | 15.96 |
| CaO | 12.17 | 12.51 | 11.23 | 16.92 | 12.10 |
| $Na_2O$ | 0.17 | 0.07 | 0.10 | 0.16 | 0.10 |
| $K_2O$ | 0.09 | 0.02 | 0.05 | 0.03 | 0.04 |
| MnO | 0.78 | 0.80 | 0.86 | 0.41 | 0.90 |
| SrO | 0.04 | 0.11 | 0.05 | 0.02 | 0.09 |
| BaO | 0.02 | 0.00 | 0.07 | 0.00 | 0.00 |
| Total | 97.53 | 97.91 | 96.42 | 95.95 | 98.20 |
| | Number of atoms on the basis of 24 oxygens | | | | |
| Si | 8.22 | 8.31 | 8.32 | 8.18 | 8.26 |
| Al | 0.00 | 0.00 | 0.00 | 0.00 | 0.00 |
| Al | 0.31 | 0.13 | 0.26 | 0.21 | 0.17 |
| Fe | 2.12 | 1.63 | 1.55 | 1.11 | 1.59 |
| Mg | 2.83 | 3.42 | 3.46 | 3.36 | 3.55 |
| Ca | 2.00 | 2.01 | 1.82 | 2.76 | 1.94 |
| Na | 0.05 | 0.02 | 0.03 | 0.05 | 0.03 |
| K | 0.02 | 0.00 | 0.01 | 0.01 | 0.01 |
| Mn | 0.10 | 0.10 | 0.11 | 0.05 | 0.11 |
| Sr | 0.00 | 0.01 | 0.00 | 0.00 | 0.01 |
| Ba | 0.00 | 0.00 | 0.00 | 0.00 | 0.00 |
| 100Mg/(Mg+Fe+Mn) | 56.03 | 66.41 | 67.58 | 74.34 | 67.62 |

| Sample no. | 81 DL-2083B | | | | |
|---|---|---|---|---|---|
| Analysis no. | 1 | 2 | 3 | 4 | 5 |
| | Major-element chemical analyses (weight percent oxides) | | | | |
| $SiO_2$ | 55.99 | 55.50 | 54.04 | 56.70 | 54.02 |
| $Al_2O_3$ | 2.50 | 2.28 | 2.76 | 1.49 | 2.95 |
| FeO | 5.54 | 6.33 | 6.71 | 5.55 | 6.33 |
| MgO | 20.56 | 20.25 | 20.30 | 21.70 | 20.25 |
| CaO | 12.19 | 12.49 | 11.52 | 11.51 | 11.99 |
| $Na_2O$ | 0.46 | 0.43 | 0.49 | 0.24 | 0.55 |
| $K_2O$ | 0.08 | 0.07 | 0.07 | 0.07 | 0.05 |
| MnO | 0.20 | 0.19 | 0.26 | 0.21 | 0.27 |
| SrO | 0.03 | 0.03 | 0.13 | 0.04 | 0.02 |
| BaO | 0.04 | 0.07 | 0.00 | 0.00 | 0.10 |
| Total | 97.59 | 97.64 | 96.28 | 97.51 | 96.53 |
| | Number of atoms on the basis of 24 oxygens | | | | |
| Si | 8.12 | 8.10 | 8.01 | 8.21 | 7.98 |
| Al | 0.00 | 0.00 | 0.00 | 0.00 | 0.02 |
| Al | 0.43 | 0.39 | 0.48 | 0.25 | 0.49 |
| Fe | 0.67 | 0.77 | 0.83 | 0.67 | 0.78 |
| Mg | 4.45 | 4.40 | 4.48 | 4.68 | 4.46 |
| Ca | 1.89 | 1.95 | 1.83 | 1.79 | 1.90 |
| Na | 0.13 | 0.12 | 0.14 | 0.07 | 0.16 |
| K | 0.01 | 0.01 | 0.01 | 0.01 | 0.01 |
| Mn | 0.04 | 0.02 | 0.03 | 0.03 | 0.03 |
| Sr | 0.00 | 0.00 | 0.01 | 0.00 | 0.00 |
| Ba | 0.00 | 0.00 | 0.00 | 0.00 | 0.01 |
| 100Mg/(Mg+Fe+Mn) | 86.24 | 84.78 | 83.90 | 86.99 | 84.63 |

Table 2. Electron microprobe analyses of adularia.

| Sample no. | 81 FC-2020A | | | | |
|---|---|---|---|---|---|
| Analysis no. | 1 | 2 | 3 | 4 | 5 |
| | Major-element chemical analyses (weight percent oxides) | | | | |
| $SiO_2$ | 65.11 | 64.23 | 65.17 | 65.39 | 65.87 |
| $Al_2O_3$ | 18.23 | 18.06 | 18.30 | 18.45 | 17.95 |
| FeO | 0.00 | 0.00 | 0.02 | 0.00 | 0.04 |
| MgO | 0.00 | 0.01 | 0.00 | 0.00 | 0.00 |
| CaO | 0.00 | 0.00 | 0.02 | 0.00 | 0.00 |
| $Na_2O$ | 0.45 | 0.42 | 0.50 | 0.41 | 0.30 |
| $K_2O$ | 15.15 | 15.34 | 15.06 | 15.74 | 15.52 |
| MnO | 0.04 | 0.00 | 0.00 | 0.04 | 0.00 |
| SrO | 0.07 | 0.04 | 0.00 | 0.03 | 0.05 |
| BaO | 0.51 | 0.65 | 0.52 | 0.71 | 0.36 |
| Total | 99.56 | 98.74 | 99.59 | 100.77 | 100.09 |
| | Number of atoms on the basis of 32 oxygens | | | | |
| Si | 12.06 | 12.03 | 12.05 | 12.01 | 12.12 |
| Al | 3.98 | 3.99 | 3.99 | 3.99 | 3.90 |
| Fe | 0.00 | 0.00 | 0.00 | 0.00 | 0.01 |
| Mg | 0.00 | 0.00 | 0.00 | 0.00 | 0.00 |
| Ca | 0.00 | 0.00 | 0.00 | 0.00 | 0.00 |
| Na | 0.16 | 0.15 | 0.18 | 0.15 | 0.11 |
| K | 3.58 | 3.67 | 3.55 | 3.69 | 3.64 |
| Mn | 0.01 | 0.00 | 0.00 | 0.01 | 0.00 |
| Sr | 0.01 | 0.00 | 0.00 | 0.00 | 0.00 |
| Ba | 0.04 | 0.05 | 0.04 | 0.05 | 0.03 |

Table 3. Electron microprobe analyses of chlorite (total iron reported as FeO).

| Sample no. | 80 COL-2058D | | | | |
|---|---|---|---|---|---|
| Analysis no. | 1 | 2 | 3 | 4 | 5 |
| | Major-element chemical analyses (weight percent oxides) | | | | |
| $SiO_2$ | 30.53 | 32.06 | 32.12 | 31.85 | 32.33 |
| $Al_2O_3$ | 19.08 | 18.51 | 17.55 | 17.61 | 17.50 |
| FeO | 11.63 | 13.32 | 12.24 | 13.25 | 13.27 |
| MgO | 22.54 | 22.93 | 23.13 | 23.09 | 22.80 |
| CaO | 0.32 | 0.27 | 0.38 | 0.35 | 0.31 |
| $Na_2O$ | 0.03 | 0.03 | 0.05 | 0.03 | 0.00 |
| $K_2O$ | 0.08 | 0.08 | 0.07 | 0.07 | 0.08 |
| MnO | 0.43 | 0.38 | 0.39 | 0.27 | 0.36 |
| SrO | 0.06 | 0.04 | 0.02 | 0.00 | 0.06 |
| BaO | 0.00 | 0.00 | 0.00 | 0.00 | 0.00 |
| Total | 84.70 | 87.62 | 85.95 | 86.52 | 86.71 |
| | Number of atoms on the basis of 28 oxygens | | | | |
| Si | 6.15 | 6.28 | 6.39 | 6.33 | 6.40 |
| Al | 1.85 | 1.72 | 1.61 | 1.67 | 1.60 |
| Al | 2.68 | 2.55 | 2.50 | 2.45 | 2.48 |
| Fe | 1.96 | 2.18 | 2.04 | 2.20 | 2.19 |
| Mg | 6.77 | 6.70 | 6.86 | 6.83 | 6.73 |
| Ca | 0.07 | 0.06 | 0.08 | 0.07 | 0.07 |
| Na | 0.01 | 0.01 | 0.02 | 0.01 | 0.00 |
| K | 0.02 | 0.02 | 0.02 | 0.02 | 0.02 |
| Mn | 0.07 | 0.06 | 0.07 | 0.05 | 0.06 |
| Sr | 0.01 | 0.01 | 0.00 | 0.00 | 0.01 |
| Ba | 0.00 | 0.00 | 0.00 | 0.00 | 0.00 |
| Fe/Fe+Mg | 0.22 | 0.25 | 0.23 | 0.24 | 0.26 |

| Sample no. | 81 CB-2011B | | | | |
|---|---|---|---|---|---|
| Analysis no. | 1 | 2 | 3 | 4 | 5 |
| | Major-element chemical analyses (weight percent oxides) | | | | |
| SiO2 | 28.22 | 29.10 | 29.06 | 28.94 | 29.40 |
| $Al_2O_3$ | 18.35 | 18.68 | 19.24 | 18.57 | 18.38 |
| FeO | 21.44 | 19.62 | 20.31 | 20.15 | 21.90 |
| MgO | 17.29 | 20.14 | 18.87 | 18.92 | 16.86 |
| CaO | 0.14 | 0.15 | 0.16 | 0.09 | 0.13 |
| $Na_2O$ | 0.01 | 0.02 | 0.02 | 0.04 | 0.00 |
| $K_2O$ | 0.08 | 0.07 | 0.17 | 0.08 | 0.14 |
| MnO | 0.57 | 0.56 | 0.47 | 0.56 | 0.57 |
| SrO | 0.04 | 0.05 | 0.06 | 0.00 | 0.07 |
| BaO | 0.04 | 0.00 | 0.00 | 0.00 | 0.00 |
| Total | 86.18 | 88.39 | 88.36 | 87.35 | 87.45 |
| | Number of atoms on the basis of 28 oxygens | | | | |
| Si | 5.93 | 5.89 | 5.90 | 5.94 | 6.07 |
| Al | 2.07 | 2.11 | 2.10 | 2.06 | 1.93 |
| Al | 2.47 | 2.34 | 2.50 | 2.43 | 2.55 |
| Fe | 3.77 | 3.32 | 3.45 | 3.46 | 3.78 |
| Mg | 5.41 | 6.07 | 5.71 | 5.79 | 5.19 |
| Ca | 0.03 | 0.03 | 0.03 | 0.02 | 0.03 |
| Na | 0.01 | 0.01 | 0.01 | 0.02 | 0.00 |
| K | 0.02 | 0.02 | 0.04 | 0.02 | 0.04 |
| Mn | 0.10 | 0.10 | 0.08 | 0.10 | 0.10 |
| Sr | 0.00 | 0.01 | 0.01 | 0.00 | 0.01 |
| Ba | 0.00 | 0.00 | 0.00 | 0.00 | 0.00 |
| Fe/Fe+Mg | 0.41 | 0.35 | 0.38 | 0.37 | 0.42 |

Table 3. continued.

| Sample no. | SUNEDCO 58-28 3220 | | | | |
|---|---|---|---|---|---|
| Analysis no. | 1 | 2 | 3 | 4 | 5 |
| | Major-element chemical analyses (weight percent oxides) | | | | |
| $SiO_2$ | 26.48 | 28.03 | 26.80 | 27.87 | 27.39 |
| $Al_2O_3$ | 15.14 | 16.63 | 16.14 | 16.12 | 16.21 |
| FeO | 24.57 | 27.73 | 28.34 | 28.58 | 27.15 |
| MgO | 10.51 | 11.14 | 11.01 | 11.21 | 11.17 |
| CaO | 0.61 | 0.77 | 0.55 | 0.74 | 0.73 |
| $Na_2O$ | 0.06 | 0.08 | 0.07 | 0.08 | 0.04 |
| $K_2O$ | 0.17 | 0.03 | 0.03 | 0.04 | 0.06 |
| MnO | 1.08 | 1.04 | 1.13 | 1.05 | 1.01 |
| SrO | 0.00 | 0.04 | 0.00 | 0.06 | 0.06 |
| BaO | 0.00 | 0.00 | 0.00 | 0.00 | 0.00 |
| Total | 78.62 | 85.49 | 84.07 | 85.75 | 83.82 |
| | Number of atoms on the basis of 24 oxygens | | | | |
| Si | 6.30 | 6.18 | 6.06 | 6.16 | 6.16 |
| Al | 1.70 | 1.82 | 1.94 | 1.84 | 1.84 |
| Al | 2.55 | 2.50 | 2.36 | 2.36 | 2.45 |
| Fe | 4.89 | 5.11 | 5.36 | 5.28 | 5.11 |
| Mg | 3.73 | 3.66 | 3.71 | 3.70 | 3.74 |
| Ca | 0.15 | 0.18 | 0.13 | 0.17 | 0.18 |
| Na | 0.03 | 0.04 | 0.03 | 0.03 | 0.02 |
| K | 0.05 | 0.01 | 0.01 | 0.01 | 0.02 |
| Mn | 0.22 | 0.19 | 0.22 | 0.20 | 0.19 |
| Sr | 0.00 | 0.01 | 0.00 | 0.01 | 0.01 |
| Ba | 0.00 | 0.00 | 0.00 | 0.00 | 0.00 |
| Fe/Fe+Mg | 0.57 | 0.58 | 0.59 | 0.59 | 0.58 |

| Sample no. | SUNEDCO 58-28 4230A | | | | |
|---|---|---|---|---|---|
| Analysis no. | 1 | 2 | 3 | 4 | 5 |
| | Major-element chemical analyses (weight percent oxides) | | | | |
| $SiO_2$ | 33.76 | 32.69 | 33.24 | 34.22 | 33.52 |
| $Al_2O_3$ | 14.44 | 13.40 | 13.16 | 13.86 | 12.98 |
| FeO | 14.18 | 14.38 | 14.87 | 13.41 | 13.79 |
| MgO | 21.01 | 18.65 | 19.04 | 20.87 | 18.84 |
| CaO | 0.84 | 0.85 | 0.90 | 0.94 | 1.20 |
| $Na_2O$ | 0.09 | 0.15 | 0.13 | 0.14 | 0.16 |
| $K_2O$ | 0.10 | 0.05 | 0.06 | 0.07 | 0.08 |
| MnO | 0.32 | 0.21 | 0.26 | 0.34 | 0.32 |
| SrO | 0.03 | 0.02 | 0.01 | 0.03 | 0.05 |
| BaO | 0.00 | 0.06 | 0.00 | 0.03 | 0.00 |
| Total | 84.77 | 80.46 | 81.67 | 83.91 | 80.94 |
| | Number of atoms on the basis of 24 oxygens | | | | |
| Si | 6.87 | 7.03 | 7.06 | 7.00 | 7.14 |
| Al | 1.13 | 0.97 | 0.94 | 1.00 | 0.86 |
| Al | 2.34 | 2.43 | 2.35 | 2.35 | 2.40 |
| Fe | 2.41 | 2.59 | 2.64 | 2.30 | 2.46 |
| Mg | 6.38 | 5.98 | 6.03 | 6.37 | 5.98 |
| Ca | 0.18 | 0.20 | 0.20 | 0.21 | 0.27 |
| Na | 0.03 | 0.06 | 0.05 | 0.05 | 0.07 |
| K | 0.03 | 0.01 | 0.02 | 0.02 | 0.02 |
| Mn | 0.06 | 0.04 | 0.05 | 0.06 | 0.06 |
| Sr | 0.00 | 0.00 | 0.00 | 0.00 | 0.01 |
| Ba | 0.00 | 0.01 | 0.00 | 0.00 | 0.00 |
| Fe/Fe+Mg | 0.27 | 0.30 | 0.30 | 0.27 | 0.29 |

Table 3. continued.

| Sample no. | SUNEDCO 58-28 4230B | | | | |
|---|---|---|---|---|---|
| Analysis no. | 1 | 2 | 3 | 4 | 5 |
| | Major-element chemical analyses (weight percent oxides) | | | | |
| $SiO_2$ | 33.49 | 33.95 | 32.28 | 33.31 | 33.75 |
| $Al_2O_3$ | 13.03 | 14.03 | 14.97 | 15.16 | 14.63 |
| FeO | 14.26 | 14.09 | 14.50 | 14.31 | 14.13 |
| MgO | 22.12 | 21.71 | 21.83 | 21.59 | 21.78 |
| CaO | 0.89 | 0.74 | 0.60 | 0.82 | 0.87 |
| $Na_2O$ | 0.14 | 0.18 | 0.15 | 0.16 | 0.10 |
| $K_2O$ | 0.07 | 0.10 | 0.10 | 0.09 | 0.09 |
| MnO | 0.24 | 0.24 | 0.21 | 0.37 | 0.22 |
| SrO | 0.07 | 0.00 | 0.00 | 0.00 | 0.03 |
| BaO | 0.02 | 0.00 | 0.11 | 0.02 | 0.04 |
| Total | 84.33 | 85.04 | 84.75 | 85.83 | 85.64 |
| | Number of atoms on the basis of 24 oxygens | | | | |
| Si | 6.88 | 6.88 | 6.61 | 6.71 | 6.80 |
| Al | 1.12 | 1.12 | 1.39 | 1.29 | 1.20 |
| Al | 2.03 | 2.23 | 2.22 | 2.31 | 2.28 |
| Fe | 2.44 | 2.39 | 2.48 | 2.41 | 2.38 |
| Mg | 6.77 | 6.56 | 6.66 | 6.48 | 6.54 |
| Ca | 0.20 | 0.16 | 0.13 | 0.17 | 0.19 |
| Na | 0.05 | 0.07 | 0.06 | 0.06 | 0.04 |
| K | 0.02 | 0.03 | 0.03 | 0.02 | 0.02 |
| Mn | 0.04 | 0.04 | 0.04 | 0.06 | 0.04 |
| Sr | 0.01 | 0.00 | 0.00 | 0.00 | 0.00 |
| Ba | 0.00 | 0.00 | 0.01 | 0.00 | 0.00 |
| Fe/Fe+Mg | 0.26 | 0.27 | 0.27 | 0.27 | 0.27 |

Table 4. Electron microprobe analyses of epidote (total iron reported as $Fe_2O_3$).

| Sample no. | 80 FC-2071C | | | | |
|---|---|---|---|---|---|
| Analysis no. | 1 | 2 | 3 | 4 | 5 |
| | Major-element chemical analyses (weight percent oxides) | | | | |
| $SiO_2$ | 37.99 | 37.35 | 39.36 | 38.32 | 37.90 |
| $Al_2O_3$ | 23.37 | 22.59 | 21.17 | 23.12 | 22.68 |
| $Fe_2O_3$ | 13.63 | 14.51 | 14.53 | 14.19 | 14.94 |
| MnO | 0.08 | 0.09 | 0.38 | 0.12 | 0.11 |
| MgO | 0.00 | 0.00 | 0.37 | 0.00 | 0.01 |
| $TiO_2$ | 0.02 | 0.05 | 0.03 | 0.00 | 0.04 |
| CaO | 23.31 | 23.13 | 21.83 | 23.15 | 23.09 |
| Total | 98.40 | 97.72 | 97.67 | 98.90 | 98.77 |
| | Number of atoms on the basis of 13 oxygens | | | | |
| Si | 3.13 | 3.11 | 3.26 | 3.14 | 3.13 |
| Al | 2.27 | 2.22 | 2.07 | 2.24 | 2.20 |
| Fe | 0.84 | 0.91 | 0.91 | 0.88 | 0.93 |
| Mn | 0.01 | 0.01 | 0.03 | 0.01 | 0.01 |
| Mg | 0.00 | 0.00 | 0.05 | 0.00 | 0.00 |
| Ti | 0.00 | 0.00 | 0.00 | 0.00 | 0.00 |
| Ca | 2.06 | 2.07 | 1.94 | 2.04 | 2.04 |
| Sample no. | 81 CB-2011B | | | | |
| Analysis no. | 1 | 2 | 3 | 4 | 5 |
| | Major-element chemical analyses (weight percent oxides) | | | | |
| $SiO_2$ | 38.22 | 38.04 | 38.54 | 37.88 | 38.27 |
| $Al_2O_3$ | 23.09 | 22.67 | 24.41 | 22.98 | 23.05 |
| $Fe_2O_3$ | 13.59 | 13.90 | 12.44 | 13.83 | 13.76 |
| MnO | 0.06 | 0.07 | 0.17 | 0.14 | 0.09 |
| MgO | 0.01 | 0.00 | 0.00 | 0.01 | 0.02 |
| $TiO_2$ | 0.20 | 0.05 | 0.07 | 0.01 | 0.06 |
| CaO | 23.20 | 23.23 | 23.42 | 22.97 | 23.15 |
| Total | 98.37 | 97.96 | 99.06 | 97.82 | 98.39 |
| | Number of atoms on the basis of 13 oxygens | | | | |
| Si | 3.15 | 3.15 | 3.14 | 3.14 | 3.15 |
| Al | 2.24 | 2.21 | 2.34 | 2.25 | 2.24 |
| Fe | 0.84 | 0.87 | 0.76 | 0.86 | 0.85 |
| Mn | 0.00 | 0.01 | 0.01 | 0.01 | 0.01 |
| Mg | 0.00 | 0.00 | 0.00 | 0.00 | 0.00 |
| Ti | 0.01 | 0.00 | 0.00 | 0.00 | 0.00 |
| Ca | 2.05 | 2.06 | 2.04 | 2.04 | 2.04 |
| Sample no. | 81 CB-2038D | | | | |
| Analysis no. | 1 | 2 | 3 | 4 | 5 |
| | Major-element chemical analyses (weight percent oxides) | | | | |
| $SiO_2$ | 38.86 | 38.53 | 38.33 | 38.46 | 38.66 |
| $Al_2O_3$ | 26.58 | 23.13 | 25.70 | 25.27 | 25.81 |
| $Fe_2O_3$ | 9.49 | 14.08 | 11.96 | 12.37 | 10.34 |
| MnO | 0.02 | 0.00 | 0.40 | 0.32 | 0.08 |
| MgO | 0.00 | 0.01 | 0.02 | 0.01 | 0.00 |
| TiO2 | 0.05 | 0.01 | 0.03 | 0.01 | 0.10 |
| CaO | 23.88 | 23.37 | 22.50 | 22.85 | 23.53 |
| Total | 98.87 | 99.13 | 98.94 | 99.29 | 98.52 |
| | Number of atoms on the basis of 13 oxygens | | | | |
| Si | 3.14 | 3.15 | 3.11 | 3.12 | 3.14 |
| Al | 2.53 | 2.23 | 2.46 | 2.42 | 2.47 |
| Fe | 0.58 | 0.87 | 0.73 | 0.75 | 0.63 |
| Mn | 0.00 | 0.00 | 0.03 | 0.02 | 0.01 |
| Mg | 0.00 | 0.00 | 0.00 | 0.00 | 0.00 |
| Ti | 0.00 | 0.00 | 0.00 | 0.00 | 0.01 |
| Ca | 2.07 | 2.05 | 1.96 | 1.98 | 2.05 |

Table 4. continued.

| Sample no. | 81 CB-2038E | | | | |
|---|---|---|---|---|---|
| Analysis no. | 1 | 2 | 3 | 4 | 5 |
| | Major-element chemical analyses (weight percent oxides) | | | | |
| $SiO_2$ | 38.48 | 38.04 | 38.04 | 38.85 | 38.29 |
| $Al_2O_3$ | 24.62 | 22.04 | 21.88 | 25.08 | 22.66 |
| $Fe_2O3$ | 12.35 | 16.10 | 14.93 | 11.51 | 14.27 |
| MnO | 0.24 | 0.05 | 0.15 | 0.14 | 0.08 |
| MgO | 0.00 | 0.01 | 0.05 | 0.00 | 0.01 |
| $TiO_2$ | 0.04 | 0.01 | 0.09 | 0.11 | 0.00 |
| CaO | 23.15 | 22.77 | 22.87 | 23.34 | 23.34 |
| Total | 98.88 | 99.02 | 98.01 | 99.03 | 98.65 |
| | Number of atoms on the basis of 13 oxygens | | | | |
| Si | 3.14 | 3.14 | 3.16 | 3.15 | 3.15 |
| Al | 2.37 | 2.14 | 2.14 | 2.40 | 2.20 |
| Fe | 0.76 | 1.00 | 0.93 | 0.70 | 0.88 |
| Mn | 0.02 | 0.00 | 0.01 | 0.01 | 0.01 |
| Mg | 0.00 | 0.00 | 0.01 | 0.00 | 0.00 |
| Ti | 0.00 | 0.00 | 0.01 | 0.01 | 0.00 |
| Ca | 2.02 | 2.01 | 2.04 | 2.03 | 2.06 |

| Sample no. | 81 DL-2082D | | | | |
|---|---|---|---|---|---|
| Analysis no. | 1 | 2 | 3 | 4 | 5 |
| | Major-element chemical analyses (weight percent oxides) | | | | |
| $SiO_2$ | 38.22 | 38.94 | 38.57 | 39.12 | 38.55 |
| $Al_2O3$ | 22.83 | 26.39 | 25.06 | 26.42 | 25.22 |
| $Fe_2O_3$ | 13.92 | 10.22 | 11.32 | 9.59 | 11.32 |
| MnO | 0.02 | 0.09 | 0.08 | 0.03 | 0.17 |
| MgO | 0.00 | 0.01 | 0.00 | 0.00 | 0.00 |
| TiO2 | 0.13 | 0.01 | 0.01 | 0.03 | 0.01 |
| CaO | 23.54 | 23.89 | 23.74 | 23.83 | 23.37 |
| Total | 98.66 | 99.55 | 98.78 | 99.02 | 98.64 |
| | Number of atoms on the basis of 13 oxygens | | | | |
| Si | 3.15 | 3.13 | 3.14 | 3.15 | 3.14 |
| Al | 2.22 | 2.50 | 2.40 | 2.51 | 2.42 |
| Fe | 0.86 | 0.62 | 0.69 | 0.58 | 0.69 |
| Mn | 0.00 | 0.01 | 0.01 | 0.00 | 0.01 |
| Mg | 0.00 | 0.00 | 0.00 | 0.00 | 0.00 |
| Ti | 0.01 | 0.00 | 0.00 | 0.00 | 0.00 |
| Ca | 2.08 | 2.06 | 2.07 | 2.06 | 2.04 |

| Sample no. | 81 DL-2092B | | | | |
|---|---|---|---|---|---|
| Analysis no. | 1 | 2 | 3 | 4 | 5 |
| | Major-element chemical analyses (weight percent oxides) | | | | |
| $SiO_2$ | 38.48 | 38.65 | 38.45 | 38.39 | 38.62 |
| $Al_2O_3$ | 23.30 | 23.13 | 23.07 | 22.24 | 23.72 |
| $Fe_2O_3$ | 13.66 | 13.75 | 14.33 | 15.26 | 12.92 |
| MnO | 0.07 | 0.10 | 0.23 | 0.16 | 0.16 |
| MgO | 0.01 | 0.02 | 0.00 | 0.02 | 0.00 |
| $TiO_2$ | 0.06 | 0.05 | 0.07 | 0.04 | 0.04 |
| CaO | 23.34 | 23.59 | 22.59 | 23.01 | 23.15 |
| Total | 98.92 | 99.29 | 98.74 | 99.12 | 98.61 |
| | Number of atoms on the basis of 13 oxygens | | | | |
| Si | 3.15 | 3.16 | 3.16 | 3.15 | 3.16 |
| Al | 2.25 | 2.23 | 2.23 | 2.15 | 2.29 |
| Fe | 0.84 | 0.84 | 0.89 | 0.94 | 0.80 |
| Mn | 0.00 | 0.01 | 0.02 | 0.01 | 0.01 |
| Mg | 0.00 | 0.00 | 0.00 | 0.00 | 0.00 |
| Ti | 0.00 | 0.00 | 0.00 | 0.00 | 0.00 |
| Ca | 2.05 | 2.06 | 1.99 | 2.03 | 2.03 |

Table 5. Electron microprobe analyses of garnet (total iron reported as $Fe_2O_3$).

| Sample no. | 80 COL-2036 | | | | |
|---|---|---|---|---|---|
| Analysis no. | 1 | 2 | 3 | 4 | 5 |
| | Major-element chemical analyses (weight percent oxides) | | | | |
| $SiO_2$ | 35.25 | 35.58 | 35.75 | 36.70 | 35.90 |
| Al2O3 | 0.23 | 0.14 | 0.24 | 0.19 | 0.07 |
| $Fe_2O_3$ | 28.99 | 29.83 | 29.53 | 29.47 | 29.73 |
| MgO | 0.32 | 0.28 | 0.42 | 0.64 | 0.16 |
| CaO | 31.32 | 31.37 | 31.66 | 32.21 | 32.64 |
| $Na_2O$ | 0.01 | 0.01 | 0.00 | 0.00 | 0.00 |
| $K_2O$ | 0.03 | 0.03 | 0.02 | 0.02 | 0.02 |
| MnO | 4.58 | 4.30 | 3.65 | 2.95 | 2.53 |
| SrO | 0.00 | 0.02 | 0.00 | 0.00 | 0.00 |
| BaO | 0.00 | 0.01 | 0.01 | 0.01 | 0.00 |
| Total | 100.73 | 101.57 | 101.53 | 102.19 | 101.05 |
| | Number of atoms on the basis of 24 oxygens | | | | |
| Si | 6.47 | 6.49 | 6.51 | 6.58 | 6.54 |
| Al | 0.05 | 0.03 | 0.05 | 0.04 | 0.02 |
| Fe | 4.01 | 4.09 | 4.05 | 3.98 | 4.08 |
| Mg | 0.09 | 0.08 | 0.11 | 0.17 | 0.04 |
| Ca | 6.16 | 6.13 | 6.18 | 6.19 | 6.37 |
| Na | 0.00 | 0.00 | 0.00 | 0.00 | 0.00 |
| K | 0.01 | 0.01 | 0.00 | 0.00 | 0.01 |
| Mn | 0.71 | 0.66 | 0.56 | 0.45 | 0.39 |
| Sr | 0.00 | 0.00 | 0.00 | 0.00 | 0.00 |
| Ba | 0.00 | 0.00 | 0.00 | 0.00 | 0.00 |

Table 6. Electron microprobe analyses of smectite (total iron reported as FeO)

| Sample no. | 80 COL-2032B | | | | |
|---|---|---|---|---|---|
| Analysis no. | 1 | 2 | 3 | 4 | 5 |
| | Major-element chemical analyses (weight percent oxides) | | | | |
| $SiO_2$ | 35.94 | 30.46 | 37.46 | 36.98 | 33.15 |
| $Al_2O_3$ | 15.64 | 9.90 | 9.31 | 8.66 | 8.56 |
| FeO | 15.65 | 21.66 | 19.40 | 20.39 | 17.99 |
| MgO | 8.89 | 6.44 | 12.14 | 11.72 | 10.12 |
| CaO | 3.20 | 3.51 | 3.05 | 2.87 | 2.12 |
| $Na_2O$ | 0.83 | 0.13 | 0.14 | 0.16 | 0.08 |
| $K_2O$ | 0.07 | 0.12 | 0.10 | 0.12 | 0.09 |
| MnO | 0.10 | 0.16 | 0.16 | 0.10 | 0.13 |
| SrO | 0.00 | 0.05 | 0.05 | 0.06 | 0.02 |
| BaO | 0.00 | 0.06 | 0.00 | 0.00 | 0.06 |
| Total | 80.32 | 72.49 | 81.79 | 81.05 | 72.32 |
| | Number of atoms on the basis of 22 oxygens | | | | |
| Si | 6.07 | 6.07 | 6.37 | 6.40 | 6.39 |
| Al | 1.93 | 1.93 | 1.63 | 1.60 | 1.61 |
| Al | 1.18 | 0.40 | 0.24 | 0.16 | 0.33 |
| Fe | 2.21 | 3.61 | 2.76 | 2.95 | 2.90 |
| Mg | 2.24 | 1.92 | 3.08 | 3.02 | 2.91 |
| Ca | 0.58 | 0.75 | 0.56 | 0.53 | 0.44 |
| Na | 0.27 | 0.05 | 0.04 | 0.54 | 0.03 |
| K | 0.01 | 0.03 | 0.02 | 0.03 | 0.02 |
| Mn | 0.01 | 0.03 | 0.02 | 0.01 | 0.02 |
| Sr | 0.00 | 0.01 | 0.00 | 0.01 | 0.00 |
| Ba | 0.00 | 0.00 | 0.00 | 0.00 | 0.00 |

| Sample no. | 88 DL-11D | | | |
|---|---|---|---|---|
| Analysis no. | 1 | 2 | 3 | 4 |
| | Major-element chemical analyses (weight percent oxides) | | | |
| $SiO_2$ | 33.69 | 28.77 | 32.30 | 35.91 |
| $Al_2O_3$ | 9.42 | 9.92 | 9.08 | 11.51 |
| FeO | 25.22 | 20.66 | 20.09 | 26.49 |
| MgO | 7.82 | 8.27 | 7.71 | 9.79 |
| CaO | 1.76 | 1.50 | 0.98 | 1.28 |
| $Na_2O$ | 0.19 | 0.14 | 0.11 | 0.20 |
| $K_2O$ | 1.08 | 0.65 | 1.74 | 1.51 |
| MnO | 0.38 | 0.45 | 0.35 | 0.48 |
| SrO | 0.05 | 0.00 | 0.05 | 0.05 |
| BaO | 0.00 | 0.06 | 0.08 | 0.12 |
| Total | 79.61 | 70.42 | 72.49 | 87.32 |
| | Number of atoms on the basis of 22 oxygens | | | |
| Si | 6.18 | 5.90 | 6.37 | 5.99 |
| Al | 1.82 | 2.10 | 1.63 | 2.01 |
| Al | 0.22 | 0.30 | 0.48 | 0.25 |
| Fe | 3.87 | 3.54 | 3.31 | 3.69 |
| Mg | 2.14 | 2.53 | 2.27 | 2.43 |
| Ca | 0.35 | 0.33 | 0.21 | 0.23 |
| Na | 0.07 | 0.55 | 0.04 | 0.06 |
| K | 0.25 | 0.17 | 0.44 | 0.32 |
| Mn | 0.06 | 0.08 | 0.06 | 0.07 |
| Sr | 0.01 | 0.00 | 0.01 | 0.00 |
| Ba | 0.00 | 0.00 | 0.01 | 0.01 |

Table 6. continued.

| Sample no. | CTGH-1 1852 | | | | |
|---|---|---|---|---|---|
| Analysis no. | 1 | 2 | 3 | 4 | 5 |
| | Major-element chemical analyses (weight percent oxides) | | | | |
| $SiO_2$ | 40.18 | 39.88 | 41.11 | 40.94 | 40.53 |
| $Al_2O3$ | 10.88 | 10.32 | 10.69 | 10.50 | 10.82 |
| FeO | 11.28 | 12.28 | 12.08 | 12.46 | 12.25 |
| MgO | 11.58 | 12.97 | 13.46 | 13.05 | 13.20 |
| CaO | 2.13 | 2.07 | 2.18 | 2.01 | 1.82 |
| $Na_2O$ | 0.16 | 0.20 | 0.20 | 0.20 | 0.17 |
| $K_2O$ | 0.16 | 0.19 | 0.29 | 0.27 | 0.24 |
| MnO | 0.24 | 0.30 | 0.20 | 0.32 | 0.37 |
| SrO | 0.00 | 0.09 | 0.10 | 0.08 | 0.01 |
| BaO | 0.09 | 0.00 | 0.00 | 0.02 | 0.11 |
| Total | 76.70 | 78.30 | 80.31 | 79.85 | 79.52 |
| | Number of atoms on the basis of 22 oxygens | | | | |
| Si | 6.85 | 6.73 | 6.74 | 6.76 | 6.72 |
| Al | 1.15 | 1.27 | 1.26 | 1.24 | 1.28 |
| Al | 1.04 | 0.78 | 0.80 | 0.80 | 0.83 |
| Fe | 1.61 | 1.73 | 1.66 | 1.72 | 1.70 |
| Mg | 2.94 | 3.26 | 3.29 | 3.21 | 3.26 |
| Ca | 0.39 | 0.37 | 0.38 | 0.35 | 0.32 |
| Na | 0.05 | 0.07 | 0.06 | 0.06 | 0.06 |
| K | 0.04 | 0.04 | 0.06 | 0.06 | 0.05 |
| Mn | 0.03 | 0.04 | 0.03 | 0.04 | 0.05 |
| Sr | 0.00 | 0.01 | 0.01 | 0.01 | 0.00 |
| Ba | 0.01 | 0.00 | 0.00 | 0.00 | 0.01 |

| Sample no. | CTGH-1 2665 | | | | |
|---|---|---|---|---|---|
| Analysis no. | 1 | 2 | 3 | 4 | 5 |
| | Major-element chemical analyses (weight percent oxides) | | | | |
| SiO2 | 44.39 | 36.54 | 35.98 | 37.30 | 36.44 |
| Al2O3 | 11.07 | 10.96 | 8.93 | 9.81 | 10.30 |
| FeO | 9.55 | 11.45 | 9.47 | 10.28 | 10.90 |
| MgO | 23.51 | 22.00 | 21.23 | 21.86 | 21.84 |
| CaO | 2.07 | 2.25 | 1.36 | 1.89 | 1.48 |
| Na2O | 0.49 | 0.43 | 0.31 | 0.39 | 0.33 |
| K2O | 0.19 | 0.11 | 0.16 | 0.13 | 0.17 |
| MnO | 0.23 | 0.37 | 0.24 | 0.21 | 0.37 |
| SrO | 0.08 | 0.08 | 0.00 | 0.00 | 0.08 |
| BaO | 0.00 | 0.00 | 0.13 | 0.00 | 0.07 |
| Total | 91.58 | 84.19 | 77.81 | 81.87 | 81.98 |
| | Number of atoms on the basis of 24 oxygens | | | | |
| Si | 6.32 | 5.82 | 6.12 | 6.04 | 5.93 |
| Al | 1.68 | 2.06 | 1.79 | 1.87 | 1.98 |
| Al | 0.18 | 0.00 | 0.00 | 0.00 | 0.00 |
| Fe | 1.14 | 1.53 | 1.35 | 1.39 | 1.48 |
| Mg | 4.99 | 5.22 | 5.38 | 5.28 | 5.30 |
| Ca | 0.32 | 0.38 | 0.25 | 0.33 | 0.26 |
| Na | 0.14 | 0.13 | 0.10 | 0.12 | 0.11 |
| K | 0.03 | 0.02 | 0.04 | 0.03 | 0.03 |
| Mn | 0.03 | 0.05 | 0.03 | 0.03 | 0.05 |
| Sr | 0.01 | 0.01 | 0.00 | 0.00 | 0.01 |
| Ba | 0.00 | 0.00 | 0.01 | 0.00 | 0.00 |

Table 7. Fluid inclusion heating and freezing data for SUNEDCO 58-28 drill-hole specimens and rock outcrop samples from the Breitenbush-Austin Hot Springs area.

| Sample depth (m) or number (yr.-no.) | Host mineral | Number of melting-point temperature measurements | Melting-point temperature $T_m$ (°C)* | Salinity (wt. % NaCl equiv-alent)*** | Number of homogenization temperature measurements | Range of homogenization temperatures $T_h$ (°C)* | Median homogenization temperature $T_h$ (°C) |
|---|---|---|---|---|---|---|---|
| 398 | Quartz | 10 | 0.0 | 0.0 | 11 | 232 - 274 | 258 |
| 882 | Calcite | 0 | -- | -- | 6 | 128 - 152 | 147 |
| 931 | " | 0 | -- | -- | 4 | 118 - 123 | 120 |
| 1360 | " | 1 | -0.1 | 0.2 | 13 | 114 - 145 | 127 |
| 1470 | " | 12 | +2.2, +3.9 | ** | 19 | 116 - 173 | 127 |
| 1794 | Anhydrite | 0 | -- | -- | 12 | 125 - 191 | 130 |
| 1910 | " | 5 | 0.0, -0.5, +1.5 | ** | 13 | 123 - 133 | 128 |
| 2347 | Primary quartz | 5 | -1.6, -1.7, -2.0 | 2.7 - 3.4 | 24 | 138 - 209 | 167 |
| 2408 | " | 4 | -2.4 | 4.0 | 11 | 202 - 216 | 210 |
| 81-80 | Quartz | 33 | -0.8 - +4.2 | ** | 46 | 92 - 220 | 148 |
| 81-81 | " | 13 | -1.7 - +2.1 | ** | 15 | 80 - 242 | 124 |
| 81-82 | " | 5 | -1.2 | 2.1 | 31 | 181 - 358 | 294 |
| 81-102 | Calcite | 4 | +0.3, +2.2 | ** | 21 | 134 - 151 | 138 |
| 81-106 | " | 24 | -0.8, -1.0, -1.3 | 1.4, 1.7, 2.2 | 59 | 78 - 196 | 159 |
| 81-120 | Quartz | 14 | -0.1, -0.2, -0.5 | 0.2, 0.4, 0.9 | 27 | 91 - 192 | 143 |

*Multiple calibration measurements, using synthetic fluid inclusions (Bodnar and Sterner, 1984) and chemical compounds with known melting-point temperatures recommended by Roedder (1984), suggest that the $T_h$ measurements should be accurate to better than ±2.0°C and that the $T_m$ values should be accurate to within ±0.2°C.
**Positive $T_m$ values indicate metastability and the fluid inclusions cannot be used for salinity calculations (Roedder, 1984).
***Salinity values are not corrected for $CO_2$.